

LA-UR-16-29185

Approved for public release; distribution is unlimited.

Title: Validation of MCNP6 Version 1.0 with the ENDF/B-VII.1 Cross Section Library for Uranium Metal, Oxide, and Solution Systems on the High Performance Computing Platform Moonlight

Author(s): Chapman, Bryan Scott
MacQuigg, Michael Robert
Wysong, Andrew Russell

Intended for: Report

Issued: 2016-12-05

Disclaimer:

Los Alamos National Laboratory, an affirmative action/equal opportunity employer, is operated by the Los Alamos National Security, LLC for the National Nuclear Security Administration of the U.S. Department of Energy under contract DE-AC52-06NA25396. By approving this article, the publisher recognizes that the U.S. Government retains nonexclusive, royalty-free license to publish or reproduce the published form of this contribution, or to allow others to do so, for U.S. Government purposes. Los Alamos National Laboratory requests that the publisher identify this article as work performed under the auspices of the U.S. Department of Energy. Los Alamos National Laboratory strongly supports academic freedom and a researcher's right to publish; as an institution, however, the Laboratory does not endorse the viewpoint of a publication or guarantee its technical correctness.



Criticality Safety Technical Document
Nuclear Criticality Safety Division

To: NCS File
Through: A. R. Wysong, NCS, E585 *ARW*
Through: B. S. Chapman, NCS, E585 *BC*
From: M. R. MacQuigg, NCS, E585 *MRM*
Phone: 505-665-7567
Email: robbie.macquigg@lanl.gov
Symbol: NCS-TECH-16-005
Date: 2016-04-21

Validation of MCNP6 Version 1.0 with the ENDF/B-VII.1 Cross Section Library for Uranium Metal, Oxide, and Solution Systems on the High Performance Computing Platform Moonlight

1. Summary

In this document, the code MCNP is validated with ENDF/B-VII.1 cross section data under the purview of ANSI/ANS-8.24-2007, for use with uranium systems¹. MCNP (Monte Carlo N-Particle) is a computer code based on Monte Carlo transport methods [1]. While MCNP has wide-reaching capability in nuclear-transport simulation, this validation is limited to the functionality related to neutron transport and calculation of criticality parameters such as k_{eff} .

The following Upper Subcritical Limit (USL) is justified within the body of this document and is subject to the Area of Applicability (AoA) defined in Section 11. It accounts for a Margin of Safety (MoS) of 0.02 and for a bounding level of bias and bias uncertainty ($b_{\text{max}} = 0.017$).

$$\text{USL}^2 = 1 - b_{\text{max}} - \text{MoS} = 0.963$$

2. Introduction

ANSI/ANS-8.1 requires that ‘*before a new operation with fissionable material is begun, or before an existing operation is changed, it shall be determined that the entire process will be subcritical under both normal and credible abnormal conditions*’ [2]. A variety of methods may be used to support that determination including application of standards-based single and multi-parameter limits, hand calculations, comparison with experimental data, in-situ measurement, and simulation using any one of a number of computer-based methods.

¹ Uranium systems including uranium metal, oxide, nitrate, and fluoride

² See Section 12. for a definition of terms and expanded discussion

| Derivative Classification Review | | |
|--|--|--|
| <input checked="" type="checkbox"/> UNCLASSIFIED <input type="checkbox"/> Export Controlled Information <input type="checkbox"/> Official Use Only <input type="checkbox"/> Unclassified Controlled Nuclear Information | <input type="checkbox"/> CONFIDENTIAL <input type="checkbox"/> Restricted Data <input type="checkbox"/> Formerly Restricted Data <input type="checkbox"/> National Security Information | <input type="checkbox"/> SECRET |
| Guidance Used: | | |
| <i>John Hargreaves/116138</i> DC/RO Name / Z Number | <i>NCSD</i> Organization | <i>John Hargreaves</i> <i>04-21-16</i> Signature Date |



Criticality Safety Technical Document
Nuclear Criticality Safety Division

To: NCS File
Through: A. R. Wysong, NCS, E585
Through: B. S. Chapman, NCS, E585
From: M. R. MacQuigg, NCS, E585
Phone: 505-665-7567
Email: robbie.macquigg@lanl.gov
Symbol: NCS-TECH-16-005
Date: 2016-04-21

Validation of MCNP6 Version 1.0 with the ENDF/B-VII.1 Cross Section Library for Uranium Metal, Oxide, and Solution Systems on the High Performance Computing Platform Moonlight

1. Summary

In this document, the code MCNP is validated with ENDF/B-VII.1 cross section data under the purview of ANSI/ANS-8.24-2007, for use with uranium systems¹. MCNP (Monte Carlo N-Particle) is a computer code based on Monte Carlo transport methods [1]. While MCNP has wide-reaching capability in nuclear-transport simulation, this validation is limited to the functionality related to neutron transport and calculation of criticality parameters such as k_{eff} .

The following Upper Subcritical Limit (USL) is justified within the body of this document and is subject to the Area of Applicability (AoA) defined in Section 11. It accounts for a Margin of Safety (MoS) of 0.02 and for a bounding level of bias and bias uncertainty ($b_{max} = 0.017$).

$$USL^2 = 1 - b_{max} - MoS = \mathbf{0.963}$$

2. Introduction

ANSI/ANS-8.1 requires that '*before a new operation with fissionable material is begun, or before an existing operation is changed, it shall be determined that the entire process will be subcritical under both normal and credible abnormal conditions*' [2]. A variety of methods may be used to support that determination including application of standards-based single and multi-parameter limits, hand calculations, comparison with experimental data, in-situ measurement, and simulation using any one of a number of computer-based methods.

¹ Uranium systems including uranium metal, oxide, nitrate, and fluoride

² See Section 12. for a definition of terms and expanded discussion

| Derivative Classification Review | | | |
|---|--|---------------------------------|------|
| <input type="checkbox"/> UNCLASSIFIED <input type="checkbox"/> Export Controlled Information <input type="checkbox"/> Official Use Only <input type="checkbox"/> Unclassified Controlled Nuclear Information | <input type="checkbox"/> CONFIDENTIAL <input type="checkbox"/> Restricted Data <input type="checkbox"/> Formerly Restricted Data <input type="checkbox"/> National Security Information | <input type="checkbox"/> SECRET | |
| Guidance Used: | | | |
| DC/RO Name / Z Number | Organization | Signature | Date |

Because uncertainty and error may exist in any of the methods, special treatments must be applied that quantify and account for those discrepancies when making a determination of subcriticality. Those treatments are part of inclusive validations that determine the overall suitability of a method for particular nuclear criticality analyses. ANSI/ANS-8.24 provides requirements and recommendations for method validation with an emphasis on computer-based methods [3].

In this document MCNP is validated and an appropriate USL is developed. The USL accounts for a bounding level of anticipated bias between MCNP predictions of neutron multiplication and that actually present in operations.

3. MCNP6

MCNP version 6.1 (here referred to as MCNP) is a computer code based on Monte Carlo transport methods that can be used for neutron transport calculations including the capability to estimate neutron multiplication factors. The code treats an arbitrary three-dimensional configuration of materials in geometric cells bounded by first and second-degree surfaces and fourth-degree elliptical tori. While MCNP has wide-reaching capability in nuclear-transport simulation [4], the discussion in this document is limited to the functionality related to neutron transport and calculation of criticality parameters such as k_{eff} .

MCNP has the capability to use a variety of cross section data including continuous and multi-group data from any of several sources. Here, only two categories of data are considered: continuous, point-wise cross section data based on the free-gas model and continuous, point-wise cross section data based on the $S(\alpha,\beta)$ model. The two models differ in the treatment of effects of collision physics with chemically bonded targets. The free-gas model ignores effects of chemical bonding and is appropriate³ when neutron energy is greater than approximately 10 eV *or* when the atomic weight of the target nucleus exceeds approximately 16. In contrast, the $S(\alpha,\beta)$ model includes effects of chemical bonding and is appropriate³ when neutron energy is less than approximately 10 eV *and* when the atomic weight of the target nucleus is less than approximately 16 [5]. Data for both categories are drawn from the ENDF/B-VII.1 evaluated nuclear data file at room temperature (293.6 K) as found in ACE data files (.80c and .20t) [6].

More detailed discussion of MCNP theory and application can be found in references 4 and 7.

4. Computer Code System

Verification of MCNP

Verification of MCNP is accomplished by executing a suite of regression-test cases provided with the distribution. The following description is found in an accompanying ‘readme’ file:

‘The regression test suite contains many short runs that serve as an MCNP code coverage tool, and may intentionally contain errors to check MCNP input processing. There are templates of expected tally and output files for each of these problems, for two different computer platforms

³ Appropriate as the treatment relates to *criticality* calculations

(Linux and Windows). When installed on any system, this suite should be run to ensure that MCNP executes correctly on that system.'

Successful verification is demonstrated by null **diff** results when comparing template outputs (generated from the code in a known, acceptable configuration) with output from the test implementation.

The regression suite was executed on the test platform and returned no significant differences. Standard output from execution of the suite and the subsequent table of **diff** results is captured in the following file:

Name: regression.log

Location: (hpss)⁴ ncs-sqm/ML/NCS-TECH-16-005/NCS-TECH-16-005.tar

md5sum⁵: 40f68a49a02b0c60eac79431d8ab31fd

Configuration Control

The computation platform (Moonlight) is a public-use system owned and operated by the HPC division. While the HPC division intentionally minimizes changes to the system, small changes such as kernel updates and hardware replacement are anticipated and are outside of the control of the NCS division. In-use testing is conducted with fixed periodicity to ensure that any changes to configuration that could potentially impact results from MCNP calculations are identified. That testing program is discussed in detail in reference 9.

Nodes of the Moonlight platform have two, eight-core Intel Xeon model E5-2670 processor chips with a base frequency of 2.6 GHz and x86-64 architecture. The operating system is the Clustered High Availability Operating System (CHAOS), a Lawrence Livermore National Laboratory-modified version of RedHat Linux

The MCNP binary is a custom build provided by the XCP division that allows for shared-memory multiprocessing. The following are file listings for the code binary and data files:

MCNP Binary

Name: mcnp6.1.0

Location: (moonlight) /usr/projects/ncs/MCNP/bin

md5sum: 90618388bc1d3fa3ca37413122ec290b

MCNP ‘xsdir’ File

Name: xsdir_mcnp6.1

Location: (moonlight) /usr/projects/ncs/Data

md5sum: 40fbf1bb0d3fc145dbcf366de5724df5

⁴ HPSS (the High Performance Storage System) is the Laboratory's archival storage system.

⁵ **md5sum** is a computer program that calculates and verifies unique 128-bit MD5 hashes [8]

MCNP Cross Section Data Files

The ENDF/B-VII.1 cross section library is comprised of a large collection of nuclide-specific files. Each cross section with a .80c or .20t reference in xsdir file has been listed in the following file:

Name: data_md5.txt

Location: (hpss) ncs-sqm/ML/NCS-TECH-16-005/NCS-TECH-16-005.tar

md5sum: 035908bf624492f6b4dc656b7ddf88c1

5. Validation Methodology

The basis of this validation is direct comparison of MCNP results with measured results for a large collection of benchmark systems from the *International Handbook of Evaluated Criticality Safety Benchmark Experiments* [10]. The benchmarks are selected for their similarities with the systems that will be subject to future evaluations. The similarities are gauged by the following attributes: elemental/nuclide composition, fissile form (i.e. metal, oxide, solution), enrichment of U-235, and ANECF and EALF as indicators of the spectrum of neutron energy in systems.

From the comparison between MCNP and measured values, appropriate bias values are derived. The collection of those bias values is then subjected to parametric and non-parametric statistical analysis to determine a bounding bias value that accounts for bias uncertainty.

6. Benchmarks

556 benchmark cases were selected drawing heavily from the WHISPER input collection [11]. Additional cases were added to extend the Area of Applicability (AoA). The 556 benchmarks correspond to systems of uranium metal, oxide, fluoride, and nitrate with 272, 186, 11, and 87 cases, respectively. Benchmarks with experimental uncertainty exceeding 0.005 were not included. This is justifiable because the exclusion did not compromise the AoA and because the inclusion of high experimental error benchmarks is fundamentally at odds with precise determination of bias. Inputs were created by members of the Nuclear Criticality Safety Division (NCSD) and members of the X Computational Physics Division (XCP) and have been heavily reviewed.

A complete list of the benchmarks used can be found in the following spreadsheet under the tab named ‘common values’.

Name: ncs-tech-16-005_analysis.xlsx

Location: (hpss) ncs-sqm/ML/NCS-TECH-16-005/NCS-TECH-16-005.tar

md5sum: 26af24fb254d31ee7487289f00bcd9a6

Table 1 provides a summary of the ranges of trending parameters observed in the benchmark set. Cross sections represented in the benchmark models are given in Tables 2 and 3 (free-gas and S(α, β), respectively). In the tables, the column “frequency” indicates the number of benchmarks that include the corresponding cross section.

Table 1 – AoA of Benchmark Collection

| Form | Parameter | Minimum | Maximum |
|-----------------|------------|---------|---------|
| all | EALF | 3.0E-08 | 8.3E-01 |
| | ANECF | 2.0E-03 | 1.5E+00 |
| | wt. % U235 | 1.3% | 97.7% |
| | H/U235 | 0.0E+00 | 2.1E+03 |
| uranium metal | EALF | 6.3E-08 | 8.3E-01 |
| | ANECF | 1.4E-02 | 1.5E+00 |
| | wt. % U235 | 1.3% | 97.7% |
| | H/U235 | 0.0E+00 | 3.9E+02 |
| uranium oxide | EALF | 5.2E-08 | 1.3E-01 |
| | ANECF | 9.7E-03 | 9.0E-01 |
| | wt. % U235 | 1.8% | 93.2% |
| | H/U235 | 0.0E+00 | 2.4E+02 |
| uranyl fluoride | EALF | 3.2E-08 | 5.1E-07 |
| | ANECF | 2.7E-03 | 5.7E-02 |
| | wt. % U235 | 4.9% | 93.2% |
| | H/U235 | 3.6E+01 | 1.4E+03 |
| uranyl nitrate | EALF | 3.0E-08 | 4.0E-07 |
| | ANECF | 2.0E-03 | 4.8E-02 |
| | wt. % U235 | 10.0% | 93.4% |
| | H/U235 | 5.5E+01 | 2.1E+03 |

Table 2 – List of Elements / Isotopes Found in Benchmarks

| Element / Isotope / Frequency | | | | | | | | | |
|-------------------------------|-------|-----|--|--|-------------|-------|-----|--|--|
| Hydrogen | 1001 | 371 | | | Zinc | 30070 | 203 | | |
| | 1002 | 9 | | | | 31069 | 1 | | |
| Lithium | 3006 | 207 | | | Gallium | 31071 | 1 | | |
| | 3007 | 205 | | | | 33075 | 6 | | |
| Beryllium | 4009 | 127 | | | Arsenic | 35079 | 2 | | |
| | 5010 | 122 | | | Bromine | 35081 | 2 | | |
| Boron | 5011 | 133 | | | | 40090 | 42 | | |
| | 6000 | 433 | | | | 40091 | 42 | | |
| Nitrogen | 7014 | 191 | | | Zirconium | 40092 | 42 | | |
| | 7015 | 176 | | | | 40094 | 42 | | |
| Oxygen | 8016 | 349 | | | | 40096 | 42 | | |
| | 8017 | 324 | | | Niobium | 41093 | 13 | | |
| Fluorine | 9019 | 22 | | | | 42092 | 121 | | |
| Sodium | 11023 | 70 | | | | 42094 | 121 | | |
| | 12024 | 231 | | | Chromium | 42095 | 121 | | |
| Magnesium | 12025 | 231 | | | | 42096 | 121 | | |
| | 12026 | 231 | | | | 42097 | 121 | | |
| Aluminum | 13027 | 320 | | | Manganese | 42098 | 121 | | |
| | 14028 | 339 | | | | 42100 | 121 | | |
| Silicon | 14029 | 339 | | | Iron | 45103 | 10 | | |
| | 14030 | 339 | | | | 47107 | 12 | | |
| Phosphorus | 15031 | 123 | | | | 47109 | 12 | | |
| | 16032 | 168 | | | Cobalt | 48106 | 79 | | |
| Sulfur | 16033 | 161 | | | | 48108 | 79 | | |
| | 16034 | 161 | | | Nickel | 48110 | 79 | | |
| | 16036 | 161 | | | | 48111 | 79 | | |
| Chlorine | 17035 | 2 | | | | 48112 | 80 | | |
| | 17037 | 2 | | | Copper | 48113 | 79 | | |
| Argon | 18036 | 14 | | | | 48114 | 79 | | |
| | 18038 | 14 | | | Zinc | 48116 | 79 | | |
| | 18040 | 14 | | | (Continued) | 50112 | 36 | | |
| Potassium | 19039 | 10 | | | | 50114 | 36 | | |
| | 19040 | 10 | | | | 50115 | 36 | | |
| | 19041 | 6 | | | | 50116 | 36 | | |

Table 3 – List of S(α, β) Cards Found in Benchmark Models

| Description / Card / Frequency | | |
|--------------------------------|------|-----|
| Beryllium in BeO | be-o | 9 |
| Beryllium in Beryllium | be | 439 |
| Carbon in Graphite | grph | 33 |
| Deuterium in Water | hwtr | 2 |
| Hydrogen in Water | lwtr | 282 |
| Oxygen in BeO | o-be | 9 |
| Hydrogen in Polyethylene | poly | 215 |

7. Execution of Benchmark Models

Benchmark model inputs were executed on moonlight using the binary and data files listed in Section 4. The input and output files are listed to the following file.

Name: io_md5.txt

Location: (hpss) ncs-sqm/ML/NCS-TECH-16-005/NCS-TECH-16-005.tar

md5sum: 267220b47a8d5de41f96306b6c961867

8. Determination of Bias

The bias between MCNP estimates of multiplication factors and that observed in corresponding experiments was calculated using Equation 1. In Equation 1, ‘n’ denotes the nth benchmark.

$$\text{bias}_n = k_{\text{eff,benchmark}_n} - k_{\text{eff,mcnp}_n} \quad \text{Equation 1}$$

The corresponding bias uncertainty was calculated using Equation 2.

$$\sigma_{\text{bias}_n} = \sqrt{\sigma_{k_{\text{eff,benchmark}_n}}^2 + \sigma_{k_{\text{eff,MCNP}_n}}^2} \quad \text{Equation 2}$$

A complete list of bias and bias uncertainty values can be found in the following spreadsheet under the tab named ‘common values’. Bias values are also presented graphically in Figures A-1 through A-20 in Appendix A (p. 16).

Name: ncs-tech-16-005_analysis.xlsx

Location: (hpss) ncs-sqm/ML/NCS-TECH-16-005/NCS-TECH-16-005.tar

md5sum: 26af24fb254d31ee7487289f00bcd9a6

9. Normality Tests

The collection of bias values was evaluated to determine if the data set, or subsets of the data, followed a normal distribution. The evaluation was done using Chi-Squared tests and quantiles dividing the distributions into 10 bins of equal integrated probability.

For the entire data set and for subsets of the data representing particular compounds (metal, oxide, uranyl nitrate, and uranyl fluoride) the set mean and standard deviation were determined using Equations 3 and 4, respectively.

$$\overline{\text{bias}} = \frac{\sum \text{bias}_n}{N} \quad \text{Equation 3}$$

$$\sigma_{\text{bias}} = \sqrt{\frac{1}{N-1} \sum (\text{bias}_n - \overline{\text{bias}})^2} \quad \text{Equation 4}$$

Bin boundaries were determined using a standard Z-table and the standard error given by Equation 4 as described by Equation 5 and 6.

$$z_i \text{ such that } P(Z \leq z_i) = P_i \quad \text{Equation 5}$$

where

$$P_i = \{0.1, 0.2, \dots, 0.9, 1.0\}$$

$$\text{bias}_{P_i} = z_i * \sigma_{\text{bias}} \quad \text{Equation 6}$$

Within the bins derived above, data was organized into histograms for comparison with the expected values of sample frequency (Chi-Squared test). The ‘test statistic’ was calculated using Equation 7 and subsequently compared to standard Chi-Squared (χ^2) values given specific degrees of freedom (DF) and P-Values. Because data were grouped into 10 bins, 9 degrees of freedom were present. A P-Value of 0.05 was selected to deliver 95 % confidence in the finding of non-normality of the data.

$$\chi^* = \sum \frac{(O-E)^2}{E} \quad \text{Equation 7}$$

where O is the *observed* frequency of data in a bin, and

E is the *expected* frequency of data in a bin

Tables B-1 through B-5 of Appendix B (p. 37) present the test parameters and results. For each data set, the Chi-Squared test statistic (χ^*) was found to exceed the acceptable value ($\chi^2=16.9$).

Because the sets of bias data failed the Chi-Squared normality test, no credit is taken for a normal distribution and alternative tests of normality will not be considered.

10. Determination of Bounding Bias

Because the bias data presented in Section 8 failed tests for normality as discussed in Section 9, a non-parametric method was used to develop a bounding bias.

The method follows closely that presented in NUREG/CR-6698 (reference 11) and has two parts. The first establishes a bounding bias and the second establishes the level of confidence that the bounding bias is truly bounding.

10.1 Bounding Bias

The NUREG methodology prescribes the selection of the lowest k_{eff} observed in the data set and its corresponding error to establish a bounding bias. It is assumed in the NUREG methodology that the bias is difference between the lowest k_{eff} less one standard deviation and 1.0. Here a minor, conservative, departure is made. Rather than finding the *minimum* k_{eff} observed, the *maximum* of $\text{bias}_n + \sigma_{\text{bias}_n}$ was found (as were calculated using Equations 1 and 2). This is different from the NUREG methodology because it finds the maximum combination of bias *and* bias uncertainty rather than the maximum bias with *subsequent* addition of corresponding bias uncertainty. Equation 8 presents the method in set notation.

$$b_{\max} = \max\{\text{bias}_n + \sigma_{\text{bias}_n}\} \quad \text{Equation 8}$$

where b_{\max} is the bounding value of bias including bias uncertainty

Bounding combinations of bias and bias uncertainty are presented in Table 4, with values corresponding to data sets for each form and for the data set as a whole (all).

Table 4 – Bounding Bias Values

| Form | b_{\max} |
|-----------------|------------|
| all | 0.017 |
| uranium metal | 0.017 |
| uranium oxide | 0.015 |
| uranyl fluoride | 0.009 |
| uranyl nitrate | 0.010 |

10.2 Confidence in Bounding Bias

NUREG/CR6698 presents a method for estimating confidence in the bounding bias that is based on binomial statistics [12]. For clarity, that method is derived here.

The binomial distribution describes the probability of ‘success’ in a series of ‘trials’ where any one trial can only result in a success or failure (hence, binomial). The number of trials is denoted by ‘n’. The probability of a success is denoted by ‘p’ and the probability of a failure is denoted by ‘q’ ($q + p = 1$). It can be shown that the probability of ‘v’ successes in n trials ($B_{n,p}(v)$) is given by Equation 9 [13, p. 229].

$$B_{n,p}(v) = \frac{n!}{v!(n-v)!} p^v q^{n-v} \quad \text{Equation 9}$$

NUREG/CR6698 uses Equation 9 to establish a level of confidence in a proposed bounding bias value. The logic is based on the assumption that the bias exhibited for each benchmark represents a random sampling of the true distribution of bias ($P(b)$). It is therefore implied that the distribution of biases well approximates a true, converged distribution of bias. The interpretation of Equation 9 in terms of bias sampling is as such: a success is defined to be a sample of bias that is greater than the bounding bias (occurring with probability p) and a failure is a sample of bias

that is bound by the bounding bias (occurring with probability q). q is equal to the cumulative probability of the bias distribution up to the bounding bias value as show in Equation 10.

$$q = \int_{-\infty}^{b_{\max}} P(b) db \quad \text{Equation 10}$$

where b_{\max} is the bounding value of bias

While $P(b)$ is not known, values of q can be tested against the data set to indicate how completely the bias distribution is bound by the bounding bias value. The case where $v = 0$ corresponds to the probability that of n samplings, no sample is found to be greater than the bounding bias. In that case, Equation 9 reduces to Equation 11

$$B_{n,p}(v = 0) = q^n \quad \text{Equation 11}$$

Equation 12 is used to estimate the probability that one or more values in the set of n values *will* exceed the bounding bias. Equation 12 is plotted as a function of q in Figure 1.

$$B_{n,p}(v > 1) = 1 - B_{n,p}(v = 0) = 1 - q^n \quad \text{Equation 12}$$

This result is equivalent to the *confidence* that the bounding bias corresponds to a cumulative probability of q or greater. Table 5 provides values associated with varied confidence levels based on 556 bias observations (n). To illustrate use of the table, consider values for the 99.6 % confidence level. In that case, there is 99.6 % confidence that 99 % of future bias values will be less than b_{\max} and, conversely, that 1 % of future bias values may be greater than b_{\max} .

Table 5 – Confidence in Bounding Bias

| Confidence | $q(b_{\max})$ | $1 - q(b_{\max})$ |
|------------|---------------|-------------------|
| 99.6 % | 99.000 % | 1.000 % |
| 75 % | 99.750 % | 0.250 % |
| 50 % | 99.875 % | 0.125 % |

$B_{n,p}(v > 1)$

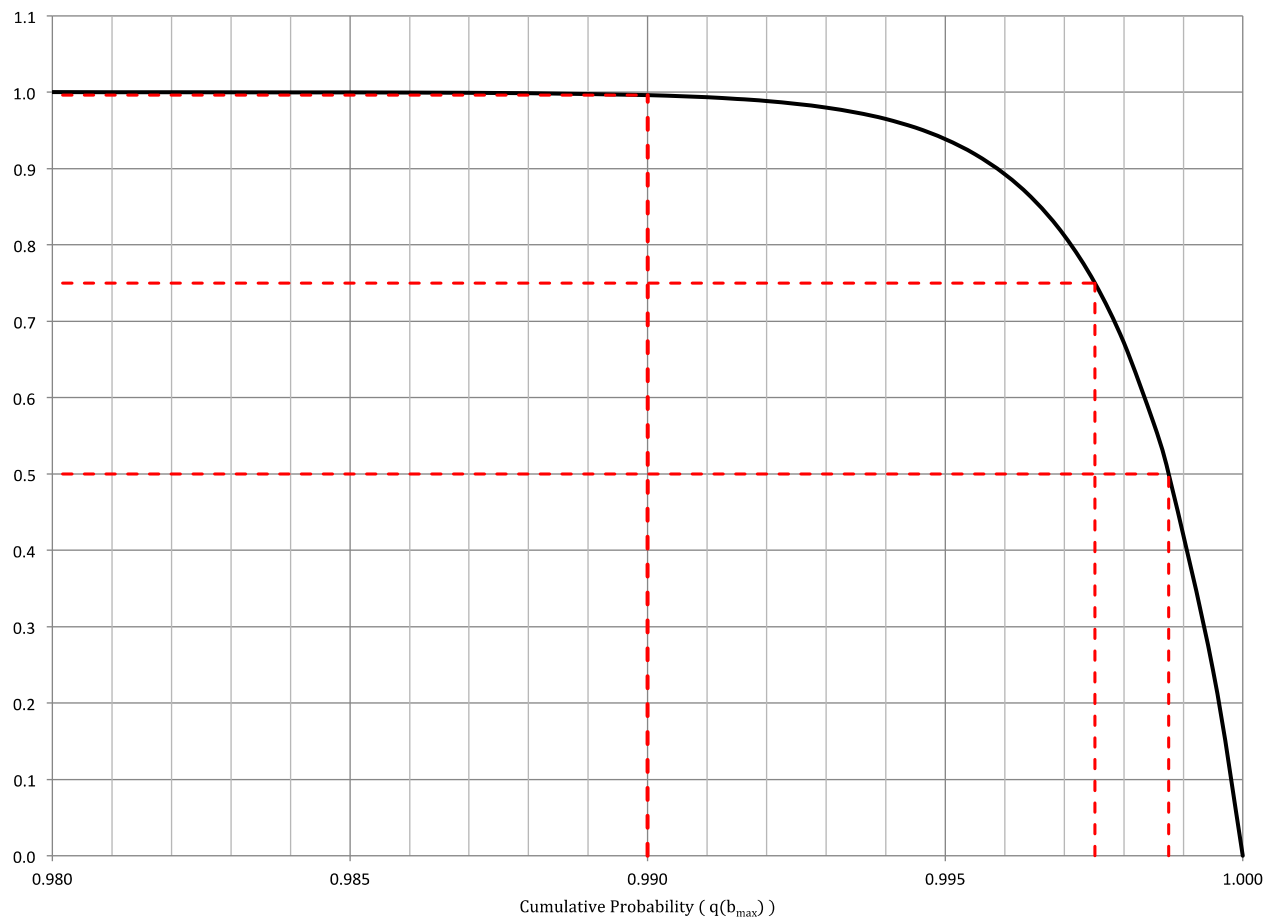


Figure 1 – Confidence in Bounding Bias

11. Trends in Bias and Determination of Area of Applicability

Trends in bias data with respect to the trending parameters (EALF, ANECF, wt. % U235, and H/U235) were evaluated visually (see Appendix A figures) and using linear least-squares fits. Higher-order fits were not considered because there are no apparent physical drivers that would correspond with, and hence justify, their application. Further, projection of higher-order fits outside of the corresponding AoA would not yield meaningful results. NUREG/CR6698 also endorses the use of linear fits [11].

Table 6 contains linear fit parameters along with interpolated and extrapolated values of bias. Within each form-specific AoA, there is no indication of a trend in bias that would exceed the bias envelope. Linear regression fits to the entire data set trend in strong agreement with the data as a function of each of the four trending parameters. Figure 2 shows the distribution of bias residuals supporting that assertion. While the distribution of residuals is not normally distributed, it is strongly biased toward zero with a slight positive skew. Because the bounding bias methodology used (see Section 10.1) captures the most extreme bias value and because the bias residual distribution indicates small probability of residuals beyond the maximum observed value, a high confidence exists in both the trend and consequently the adequacy of the bounding bias value.

Because the subsets of data form a predictable superset, the acceptable range of trending parameters (ranges considered to be part of the AoA) for each material form are taken to be that of the entire data set. The AoA for uranium systems of metal, oxide, nitrate and fluoride is therefore defined to be the range of parameters listed in Table 6 (an excerpt from Table 1, “all”) and the set of materials presented in Table 2.

Table 6 – AoA, Parameter Ranges

| Parameter | Minimum | Maximum |
|------------|---------|---------|
| EALF | 3.0E-08 | 8.3E-01 |
| ANECF | 2.0E-03 | 1.5E+00 |
| wt. % U235 | 1.3% | 97.7% |
| H/U235 | 0.0E+00 | 2.1E+03 |

12. Determination of USL

A general USL for uranium systems (metal, oxide, nitrate, fluoride) is calculated using Equation 13. In the equation, b_{max} is taken to be the maximum observed in the entire data set.

$$\begin{aligned} USL &= 1 - b_{max} - MoS - MoA \\ &= 1 - 0.017 - 0.02 - 0 = \mathbf{0.963} \end{aligned} \quad \text{Equation 13}$$

where b_{max} is the bounding value of bias including bias uncertainty

MoS is the margin of subcriticality (0.02)

MoA is the margin of applicability (0 within the AoA defined in Section 11.)

An appropriate USL for any system outside of the AoA presented here (Section 11.) requires application of an appropriate margin of applicability (MoA). See discussion of MoS and MoA in the following subsections.

Because the USL derived here applies to k_{eff} values as determined by a probabilistic method (MCNP), it will necessarily be compared to k_{eff} estimates with associated statistical uncertainty. Equation 14 demonstrates the minimum acceptable criteria for k_{eff} and its uncertainty when making a determination of subcriticality.

$$k_{\text{eff,MCNP}} + 2\sigma_{k_{\text{eff,MCNP}}} \leq \text{USL} \quad \text{Equation 14}$$

where $k_{\text{eff,MCNP}}$ is the well converged value of k_{eff} reported by MCNP

$\sigma_{k_{\text{eff,MCNP}}}$ is the standard deviation of the k_{eff} value reported MCNP

12.1 Margin of Subcriticality (MoS)

The administrative margin of subcriticality (MoS) is required by ANSI/ANS-8.24-2007. The standard discusses the requirements of that margin as follows:

“A margin of subcriticality shall be applied that is sufficiently large to ensure that calculated conditions will actually be subcritical. The selection of a margin of subcriticality should take into account the sensitivity of the system or process to variations in fissile form, geometry, or other physical characteristics. A single margin might not be appropriate over the entire validation applicability.”

The Nuclear Criticality Safety division defines that margin as a sum of margins for the following considerations: 0.005 for nuclear data uncertainty, 0.005 for potential undiscovered errors in the computation software, and an additional 0.01 for conservatism, for a total of 0.02 [14].

12.2 Margin of Applicability (MoA)

The margin of applicability (MoA)⁶ is defined here as additional margin in the USL intended to compensate for the lack of characterization outside of the defined area of applicability (AoA) (see Section 11.). An appropriate margin is determined on a case-by-case basis depending on the nature of the departure from the AoA. However, in any case, the MoA must be adequate to ensure that calculated conditions will be subcritical when the bounding bias and the MoS can't be argued to collectively bound uncertainty of a result.

12.3 Validation Cautions of Use

The following cautions are applicable to this validation.

- Not all nuclides (stable or radioactive) of any given element are necessarily included in the validation. If modeling nuclides not included in this validation additional margin or sensitivity analyses may be required.
- Isotopes not included with a high frequency within the set of modeled benchmarks may require additional margin. For example, only one benchmark critical experiment case includes U-233 as a fissionable material. The frequency of isotope inclusion within the modeled benchmarks can be found in Table 2.

It is ultimately the responsibility of the analyst to ensure that a system being analyzed is within the scope of this validation. Careful consideration is required when this determination is being made.

⁶ MoA may also be found referred to as “Applicability Margin” or “AoA”

Table 7 – Linear Fit Parameters and Bias Projections

| Form | Parameter | Y-Intercept | Slope | Projected Bias at Form Min | Projected Bias at Form Max |
|-----------------|------------|-------------|-----------|----------------------------|----------------------------|
| all | EALF | 3.13E-05 | -1.00E-03 | 0.000 | -0.001 |
| | ANECF | 2.64E-04 | -7.31E-04 | 0.000 | -0.001 |
| | wt. % U235 | 6.85E-04 | -1.49E-03 | 0.001 | -0.001 |
| | H/U235 | -2.63E-04 | 5.71E-07 | 0.000 | 0.001 |
| uranium metal | EALF | -1.39E-03 | 1.06E-03 | -0.001 | 0.000 |
| | ANECF | -3.46E-03 | 2.18E-03 | -0.003 | 0.000 |
| | wt. % U235 | -1.03E-03 | 1.62E-04 | -0.001 | -0.001 |
| | H/U235 | -8.70E-04 | -1.02E-05 | -0.001 | -0.005 |
| uranium oxide | EALF | 3.04E-04 | -1.92E-02 | 0.000 | -0.002 |
| | ANECF | -1.79E-04 | 2.83E-03 | 0.000 | 0.002 |
| | wt. % U235 | 9.59E-04 | -7.45E-03 | 0.001 | -0.006 |
| | H/U235 | 3.76E-04 | -4.75E-06 | 0.000 | -0.001 |
| uranyl fluoride | EALF | 7.89E-05 | -6.93E+03 | 0.000 | -0.003 |
| | ANECF | -1.10E-03 | 1.71E-02 | -0.001 | 0.000 |
| | wt. % U235 | 5.17E-03 | -7.68E-03 | 0.005 | -0.002 |
| | H/U235 | -1.65E-03 | 1.56E-06 | -0.002 | 0.001 |
| uranyl nitrate | EALF | -2.26E-04 | 7.87E+03 | 0.000 | 0.003 |
| | ANECF | -6.75E-04 | 7.40E-02 | -0.001 | 0.003 |
| | wt. % U235 | 4.67E-04 | 8.34E-04 | 0.001 | 0.001 |
| | H/U235 | 1.55E-03 | -8.63E-07 | 0.002 | 0.000 |

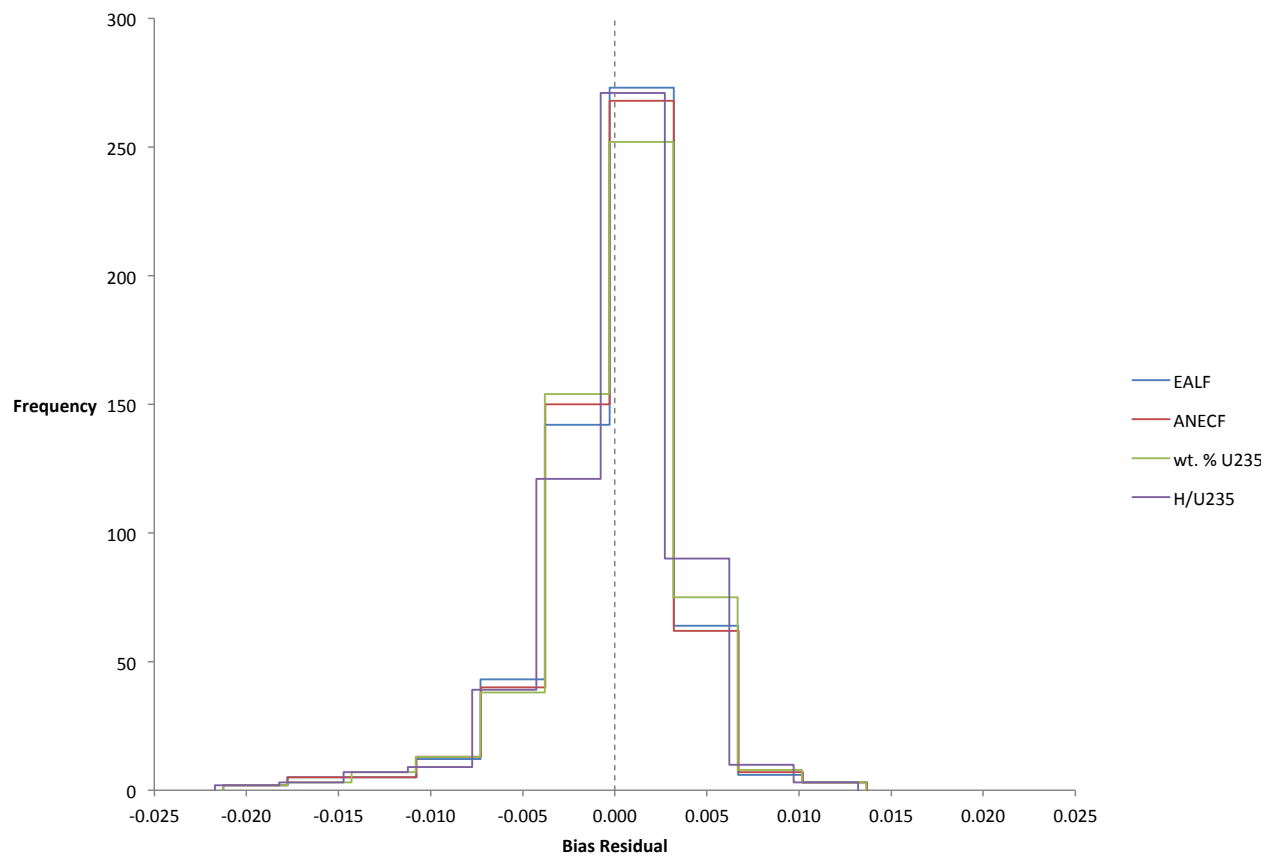


Figure 2 – Histogram of Bias Residuals, Complete Data Set, Various Trending Parameters

APPENDIX A – Graphic Representations of Bias Data

Table of Figures

| | |
|--|----|
| Figure A-1 – Bias as a Function of H/U235 Ratio, All Benchmarks | 17 |
| Figure A-2 – Bias as a Function of H/U235 Ratio, Metal Benchmarks | 18 |
| Figure A-3 – Bias as a Function of H/U235 Ratio, Oxide Benchmarks..... | 19 |
| Figure A-4 – Bias as a Function of H/U235 Ratio, Nitrate Benchmarks | 20 |
| Figure A-5 – Bias as a Function of H/U235 Ratio, Fluoride Benchmarks | 21 |
| Figure A-6 – Bias as a Function of U235 Enrichment, All Benchmarks | 22 |
| Figure A-7 – Bias as a Function of U235 Enrichment, Metal Benchmarks | 23 |
| Figure A-8 – Bias as a Function of U235 Enrichment, Oxide Benchmarks..... | 24 |
| Figure A-9 – Bias as a Function of U235 Enrichment, Nitrate Benchmarks | 25 |
| Figure A-10 – Bias as a Function of U235 Enrichment, Fluoride Benchmarks | 26 |
| Figure A-11– Bias as a Function of ANECF, All Benchmarks | 27 |
| Figure A-12 – Bias as a Function of ANECF, Metal Benchmarks..... | 28 |
| Figure A-13 – Bias as a Function of ANECF, Oxide Benchmarks | 29 |
| Figure A-14 – Bias as a Function of ANECF, Nitrate Benchmarks | 30 |
| Figure A-15 – Bias as a Function of ANECF, Fluoride Benchmarks | 31 |
| Figure A-16 – Bias as a Function of EALF, All Benchmarks | 32 |
| Figure A-17 – Bias as a Function of EALF, Metal Benchmarks..... | 33 |
| Figure A-18 – Bias as a Function of EALF, Oxide Benchmarks | 34 |
| Figure A-19 – Bias as a Function of EALF, Nitrate Benchmarks | 35 |
| Figure A-20 – Bias as a Function of EALF, Fluoride Benchmarks..... | 36 |

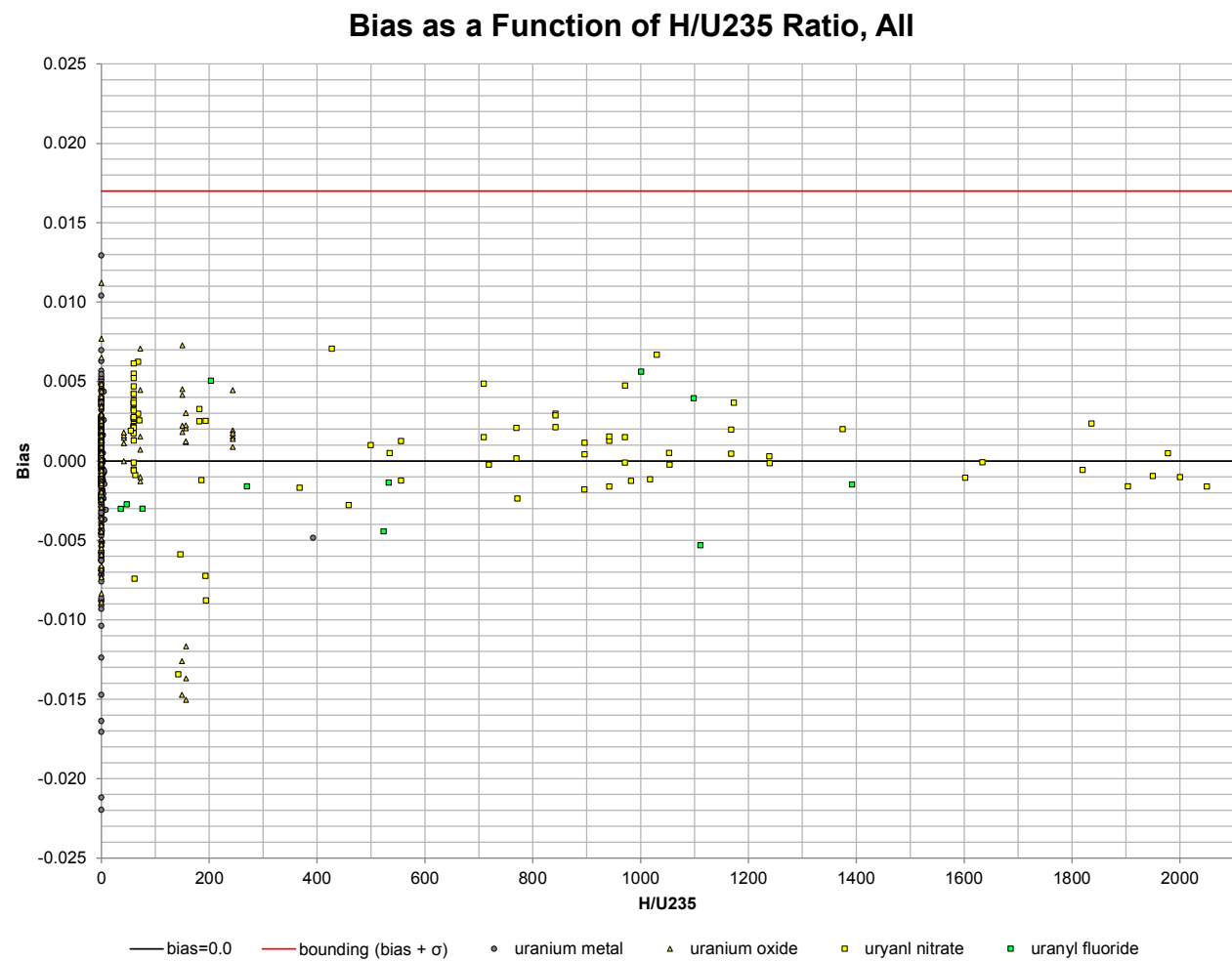
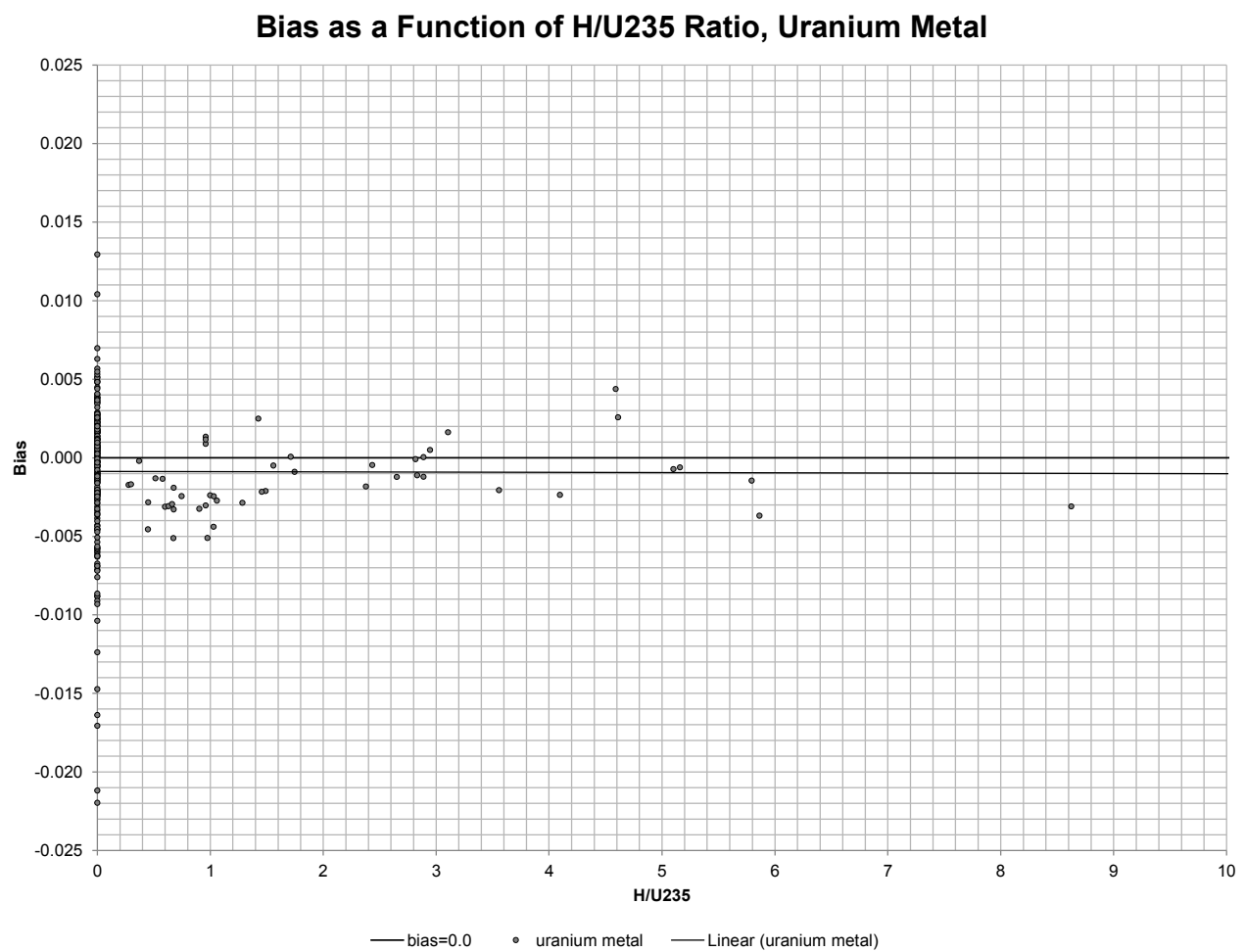


Figure A-1 – Bias as a Function of H/U235 Ratio, All Benchmarks



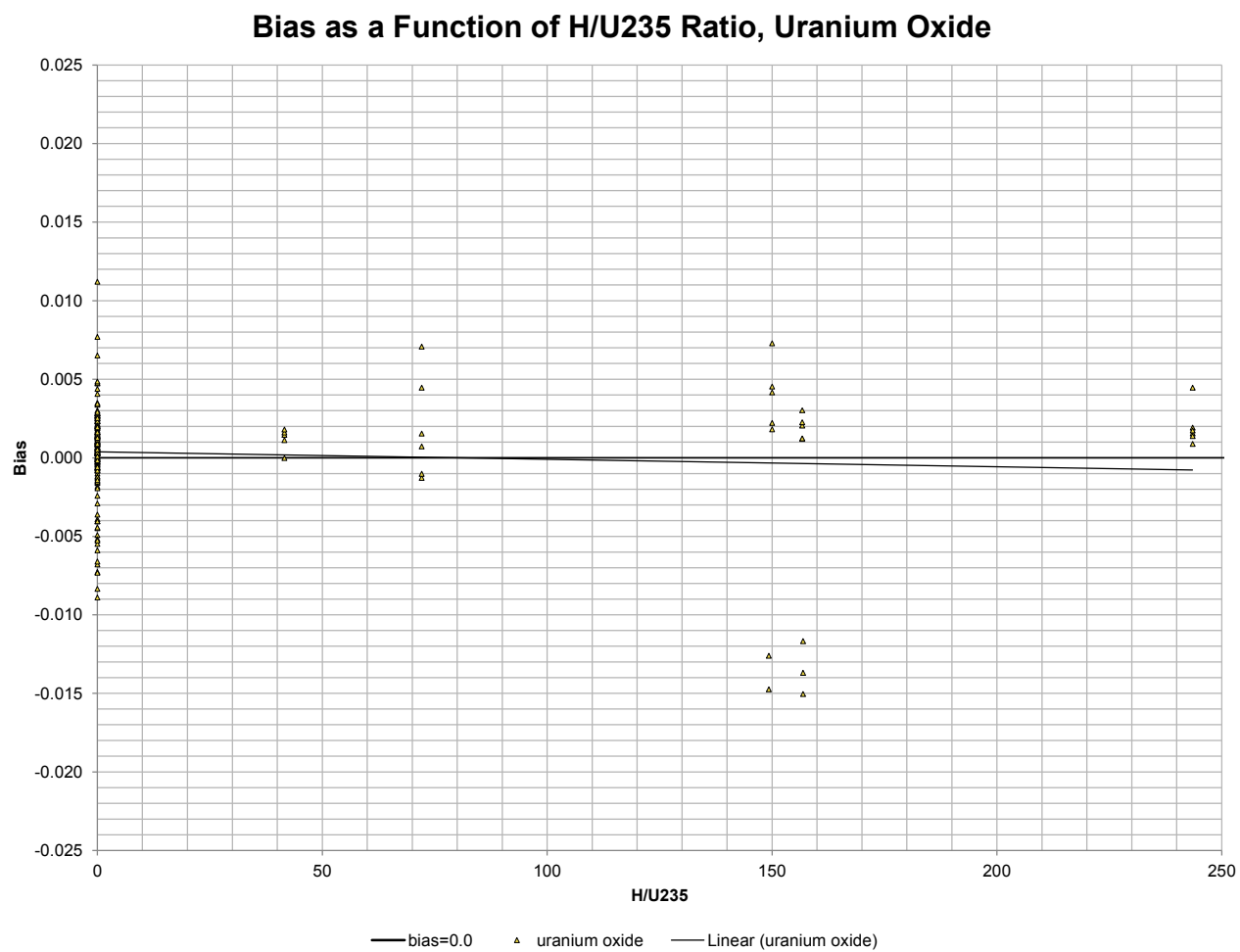


Figure A-3 – Bias as a Function of H/U235 Ratio, Oxide Benchmarks

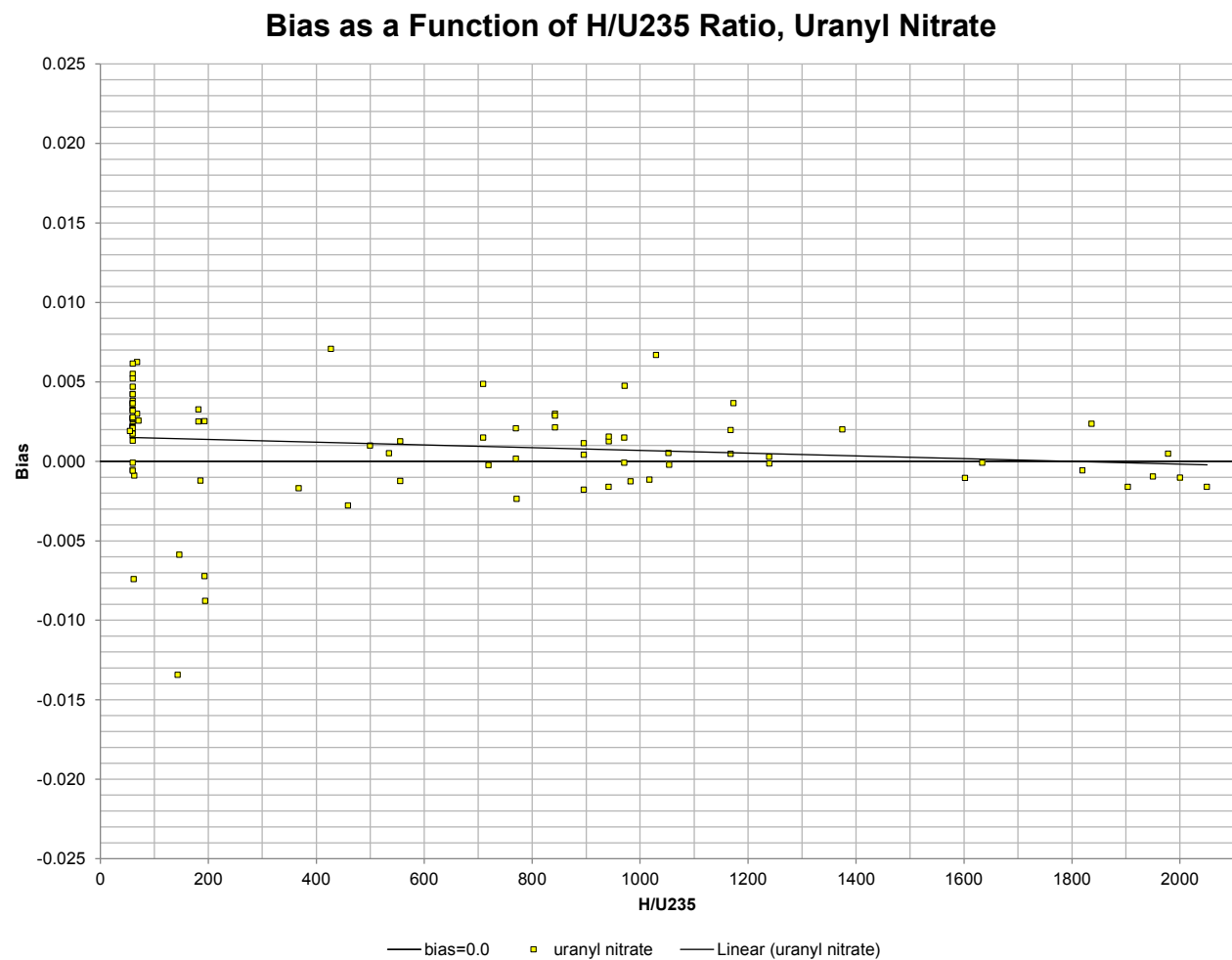


Figure A-4 – Bias as a Function of H/U235 Ratio, Nitrate Benchmarks

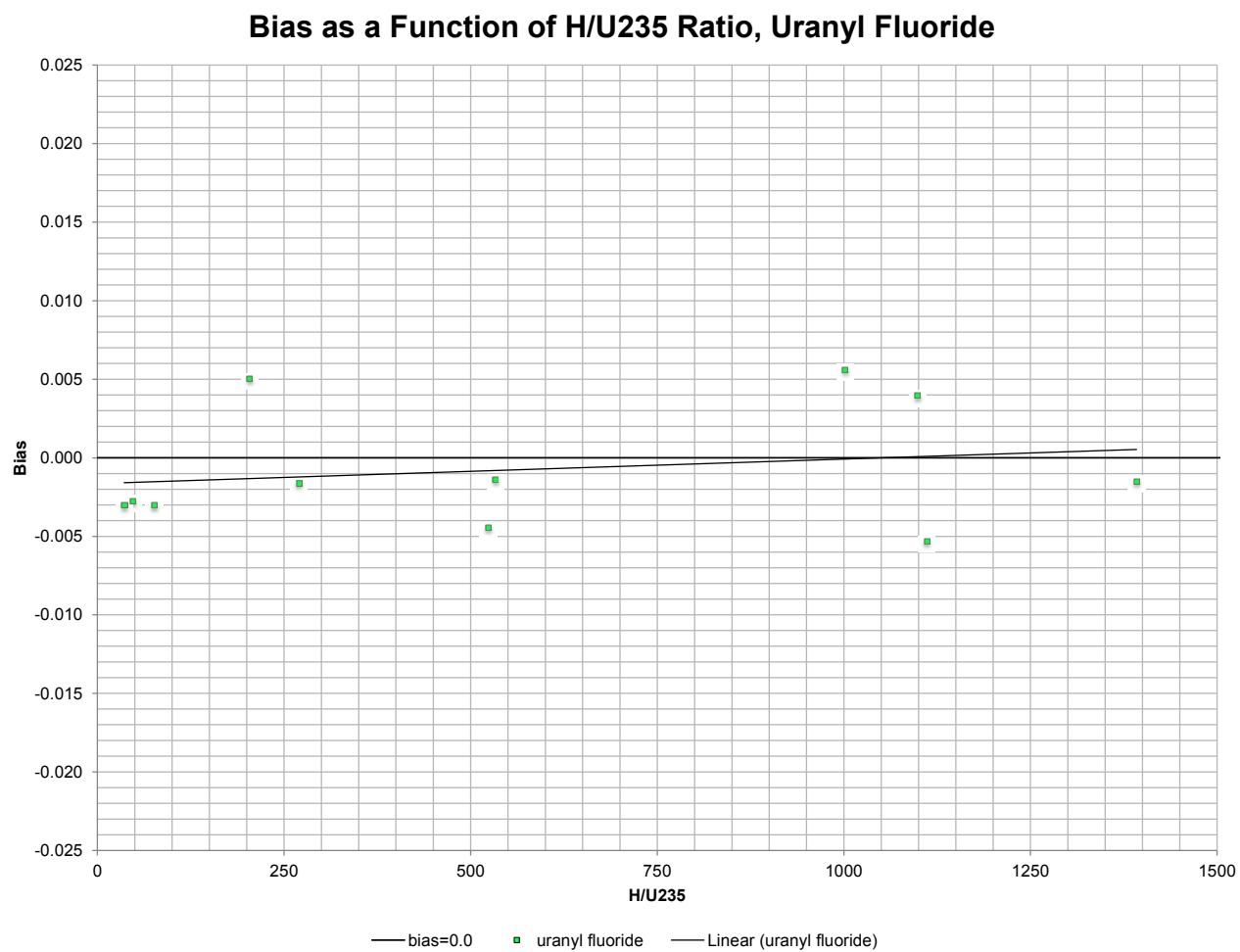


Figure A-5 – Bias as a Function of H/U235 Ratio, Fluoride Benchmarks

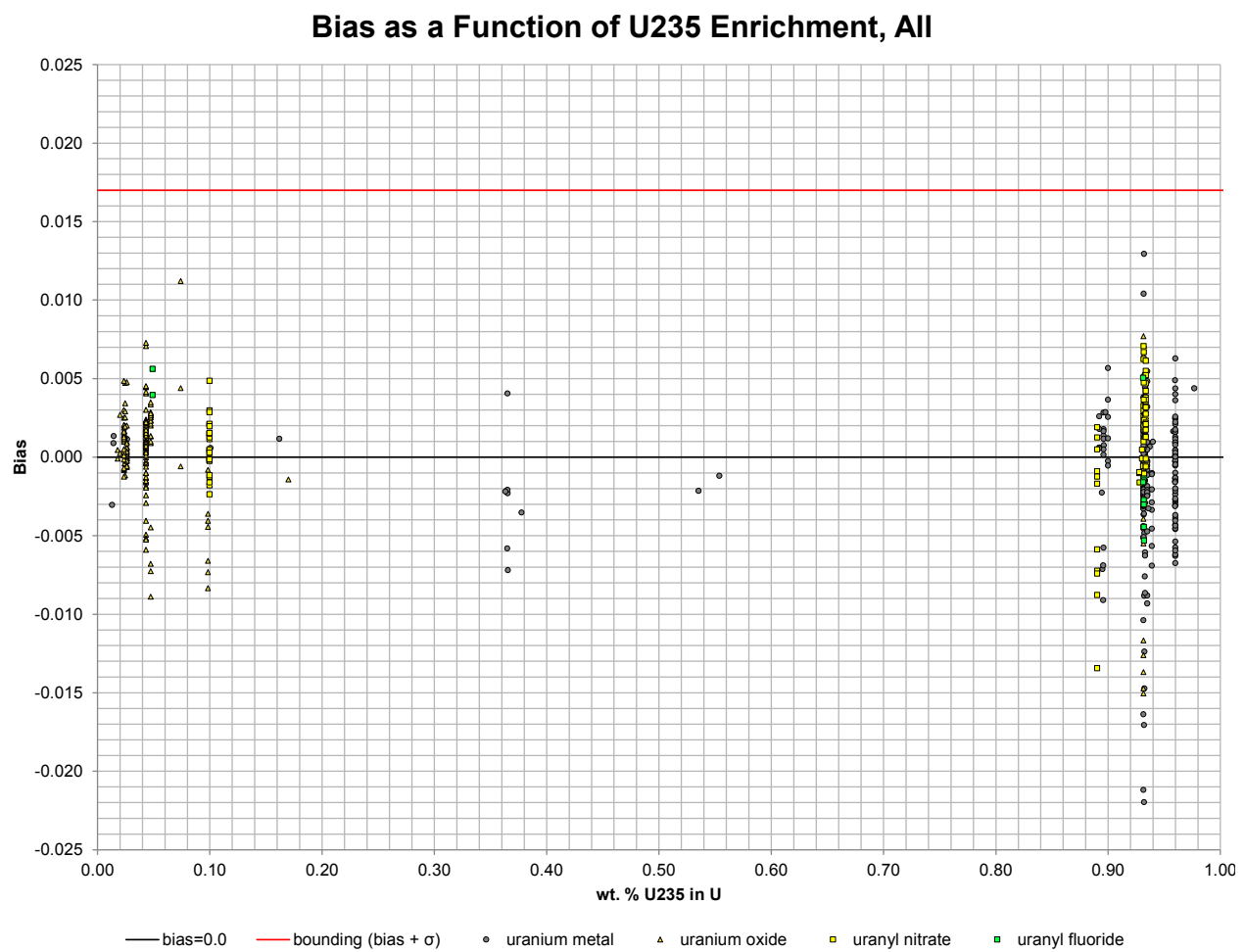


Figure A-6 – Bias as a Function of U235 Enrichment, All Benchmarks

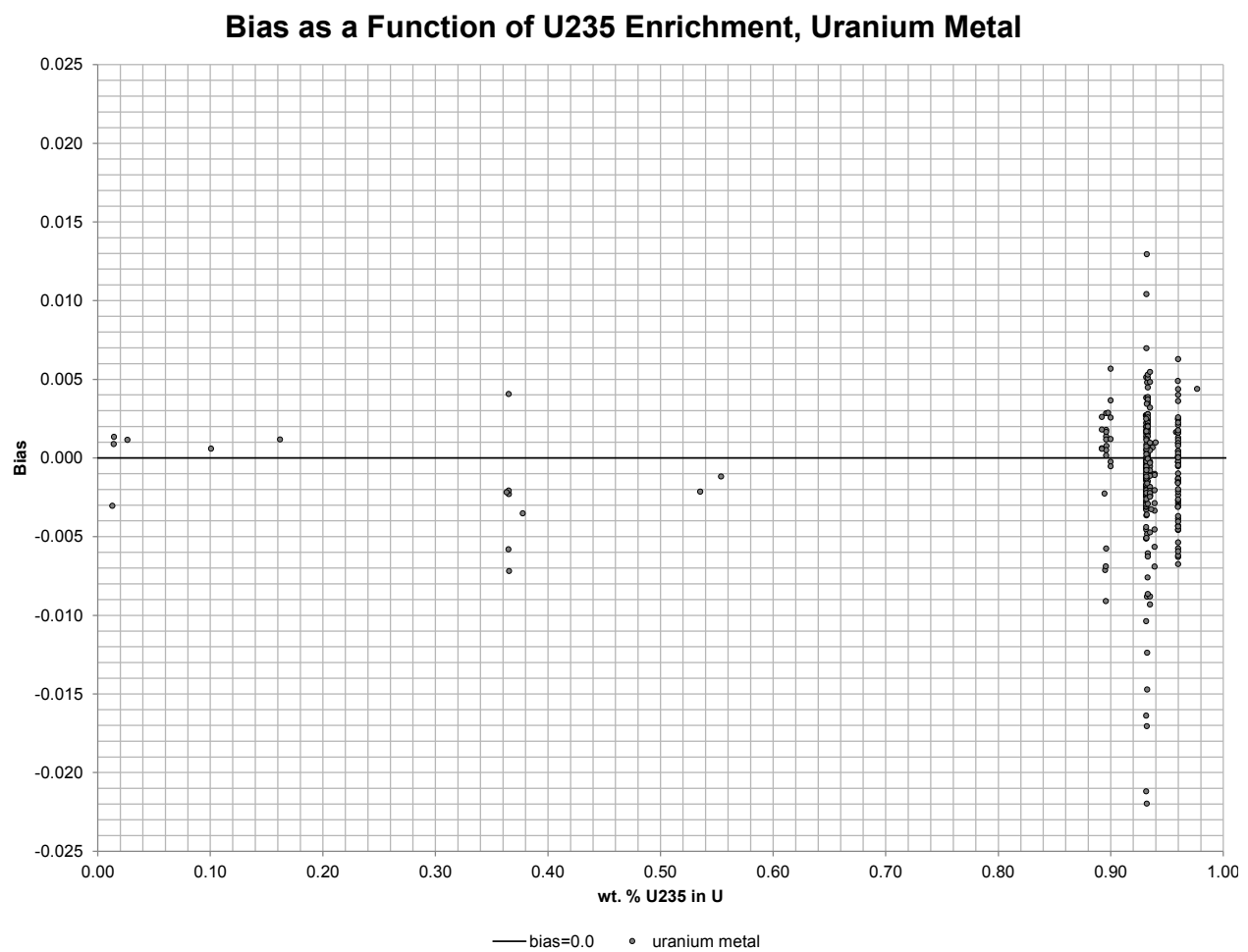


Figure A-7 – Bias as a Function of U235 Enrichment, Metal Benchmarks

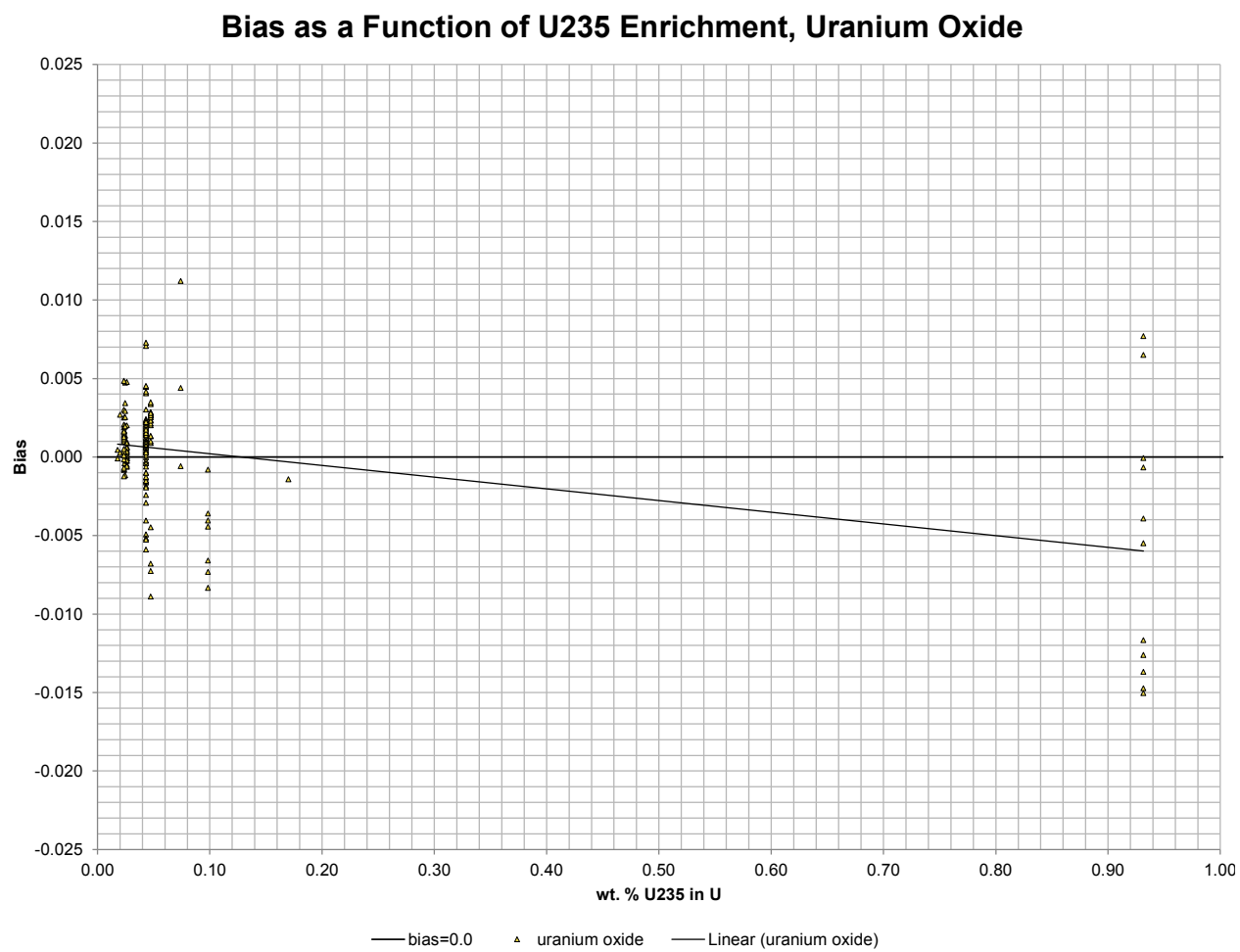


Figure A-8 – Bias as a Function of U235 Enrichment, Oxide Benchmarks

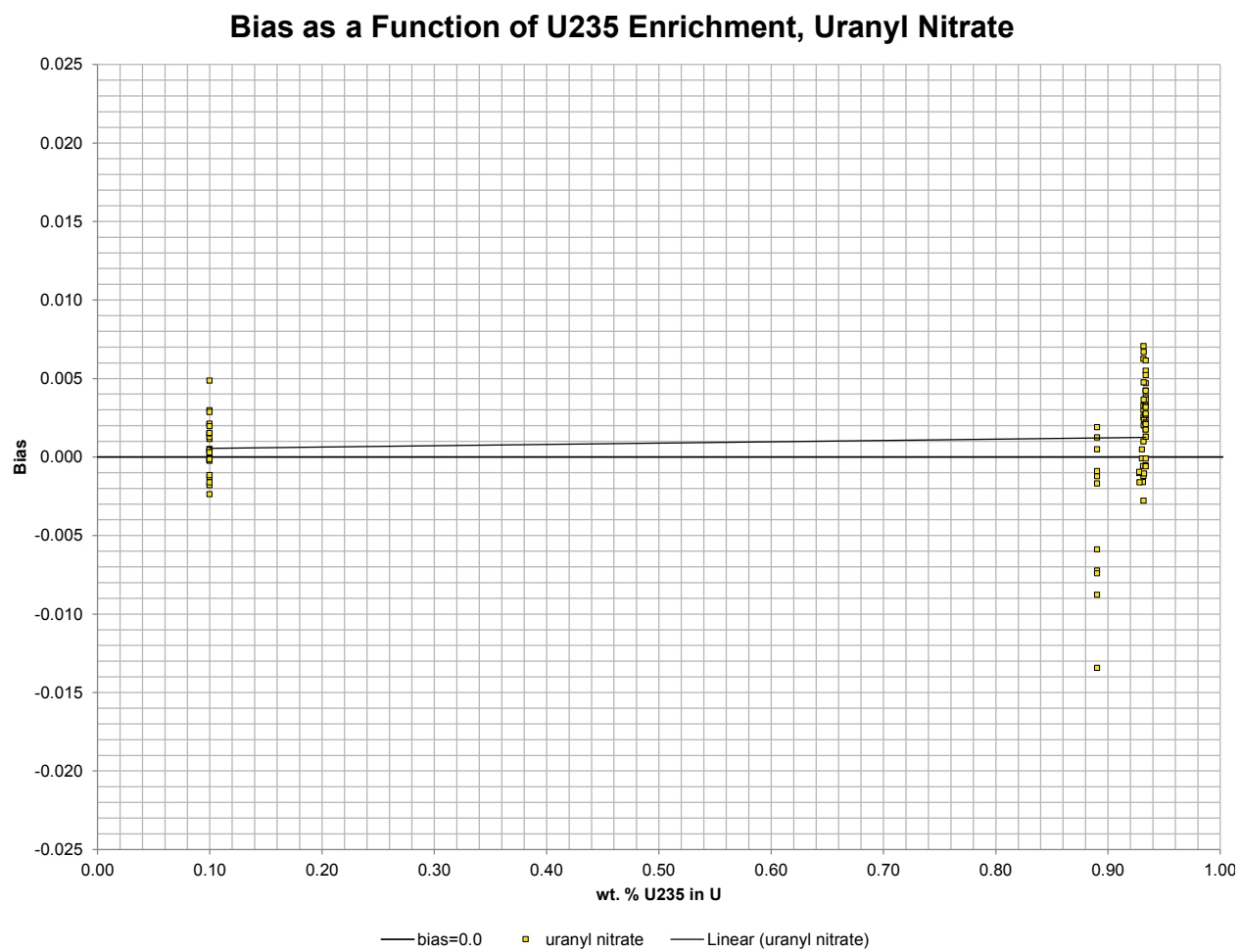


Figure A-9 – Bias as a Function of U235 Enrichment, Nitrate Benchmarks

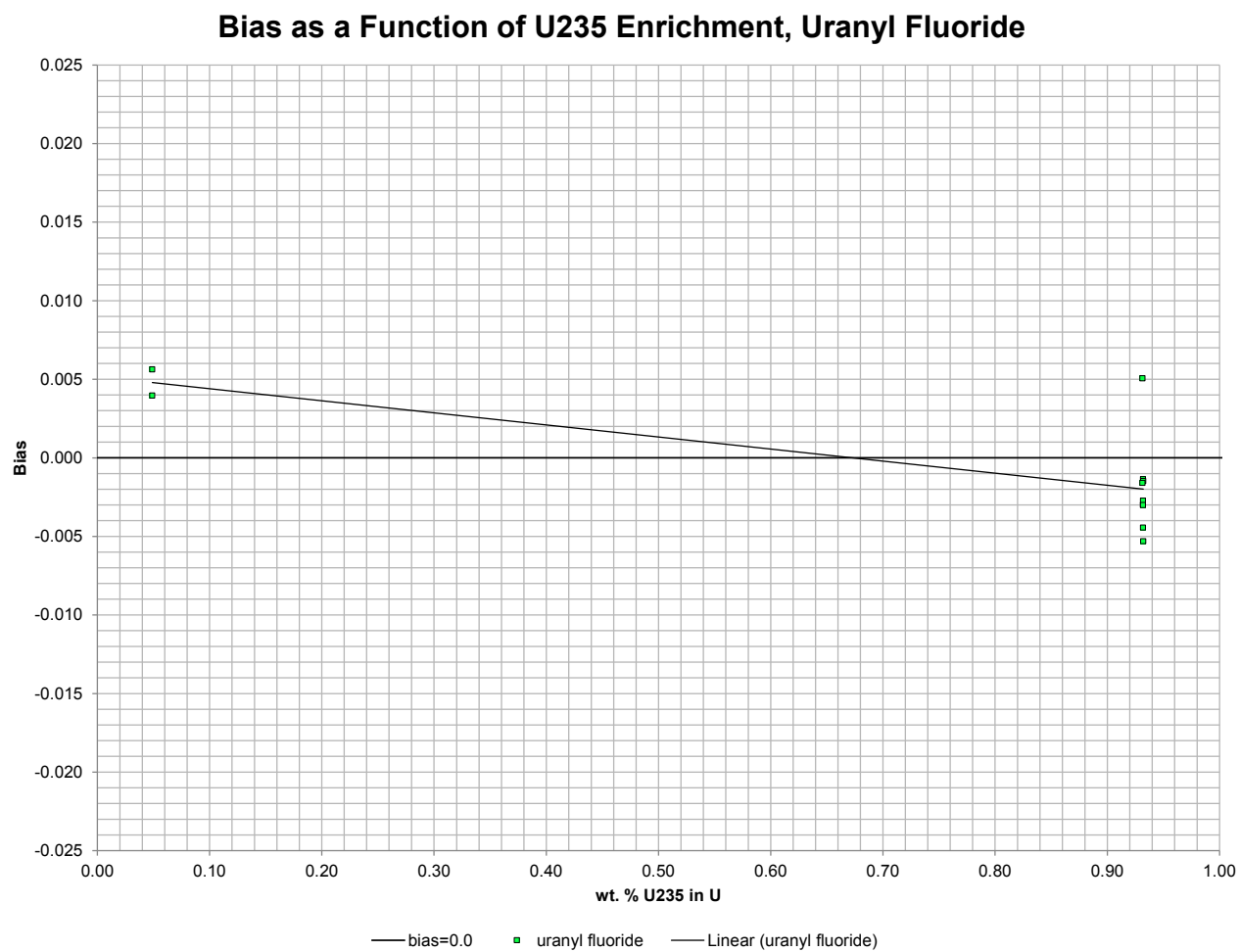


Figure A-10 – Bias as a Function of U235 Enrichment, Fluoride Benchmarks

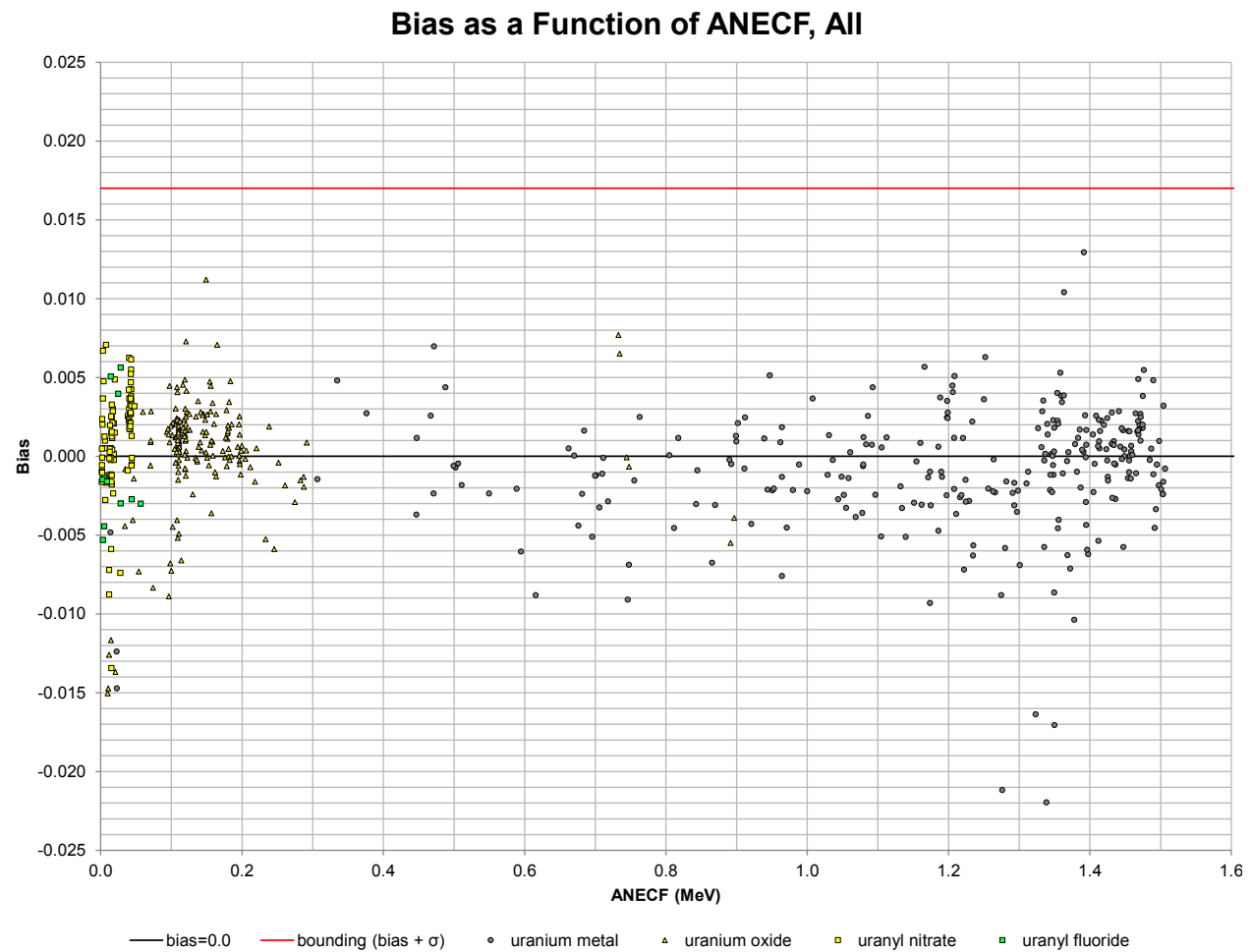


Figure A-11 – Bias as a Function of ANECF, All Benchmarks

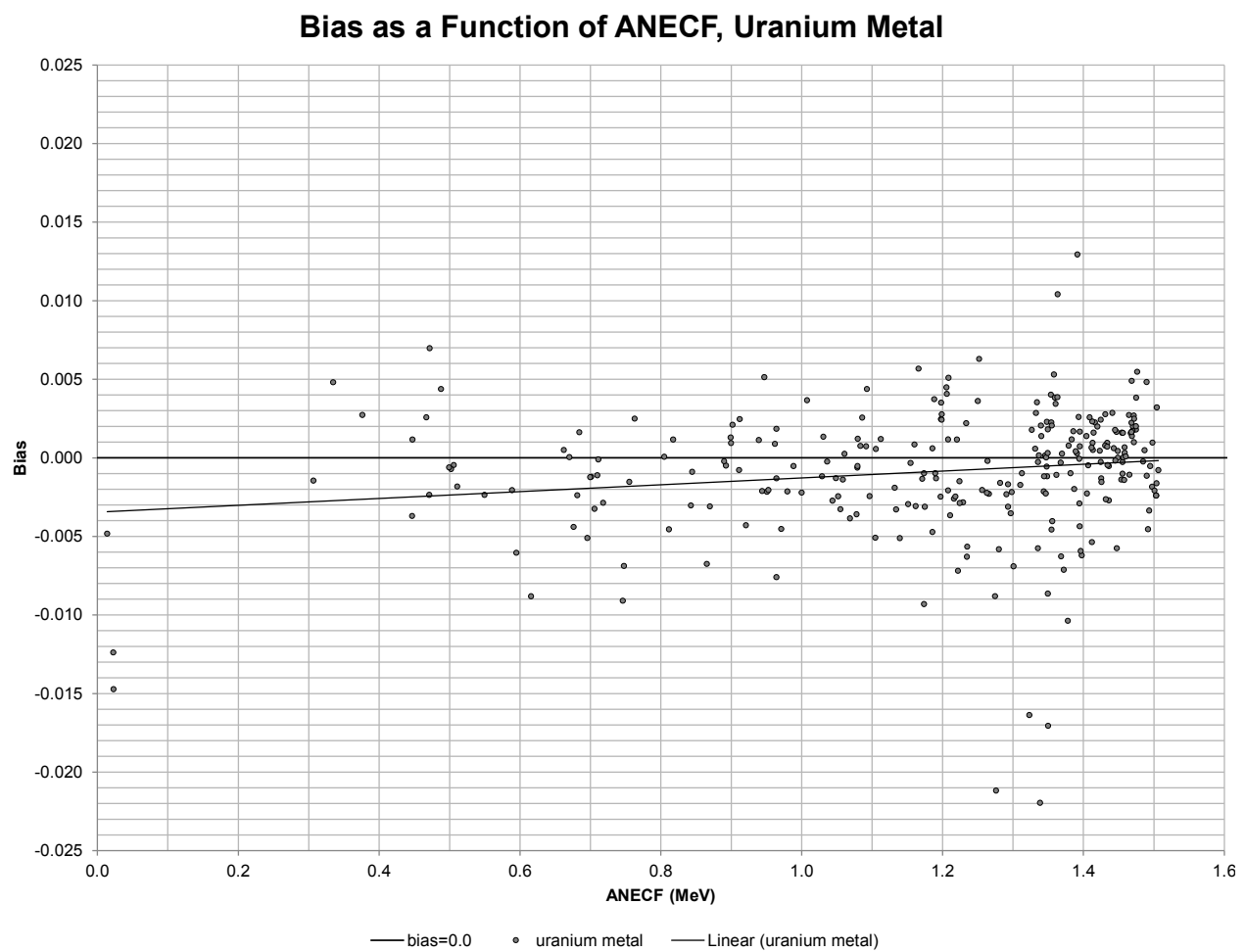


Figure A-12 – Bias as a Function of ANECF, Metal Benchmarks

Bias as a Function of ANECF, Uranium Oxide

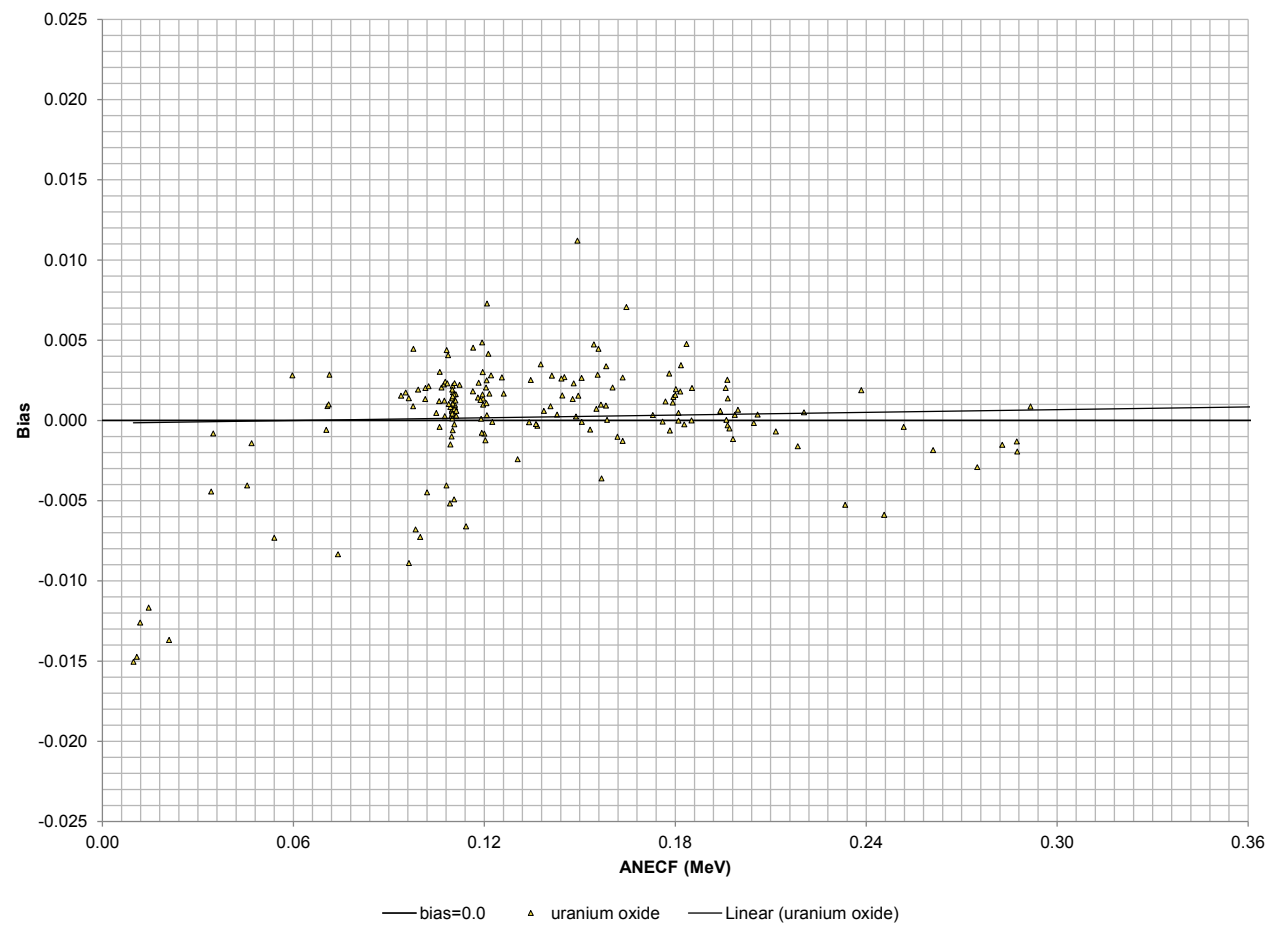
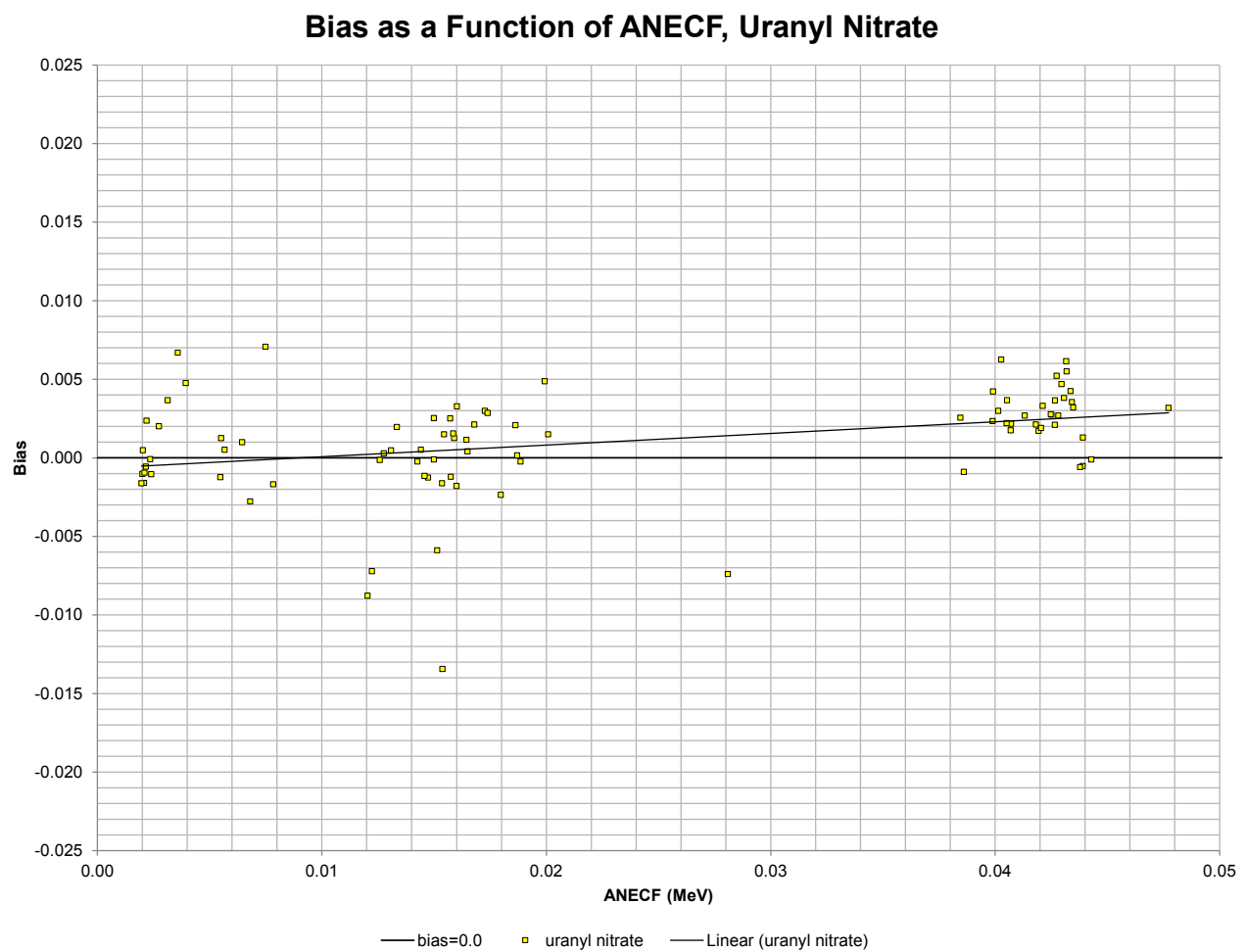


Figure A-13 – Bias as a Function of ANECF, Oxide Benchmarks



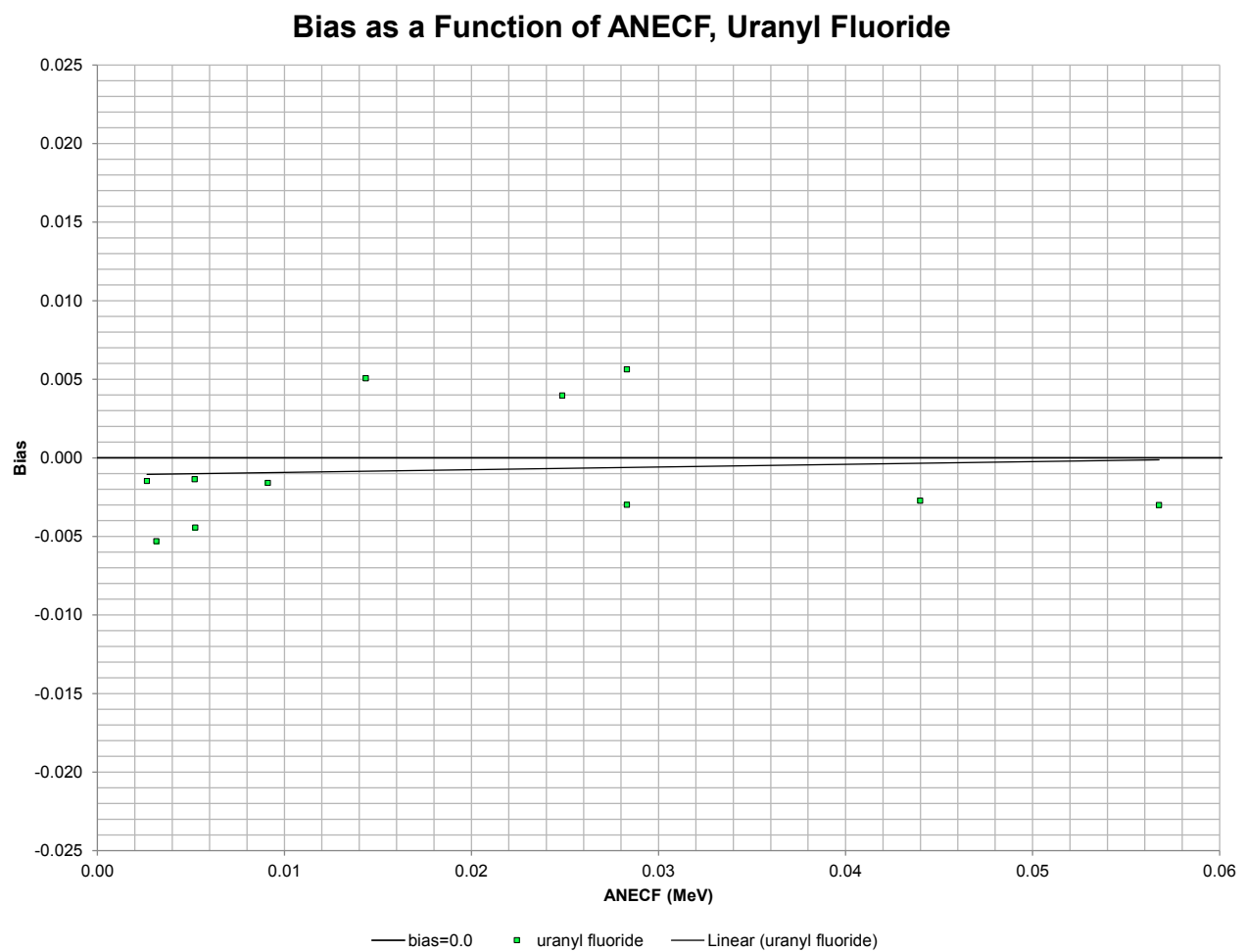


Figure A-15 – Bias as a Function of ANECF, Fluoride Benchmarks

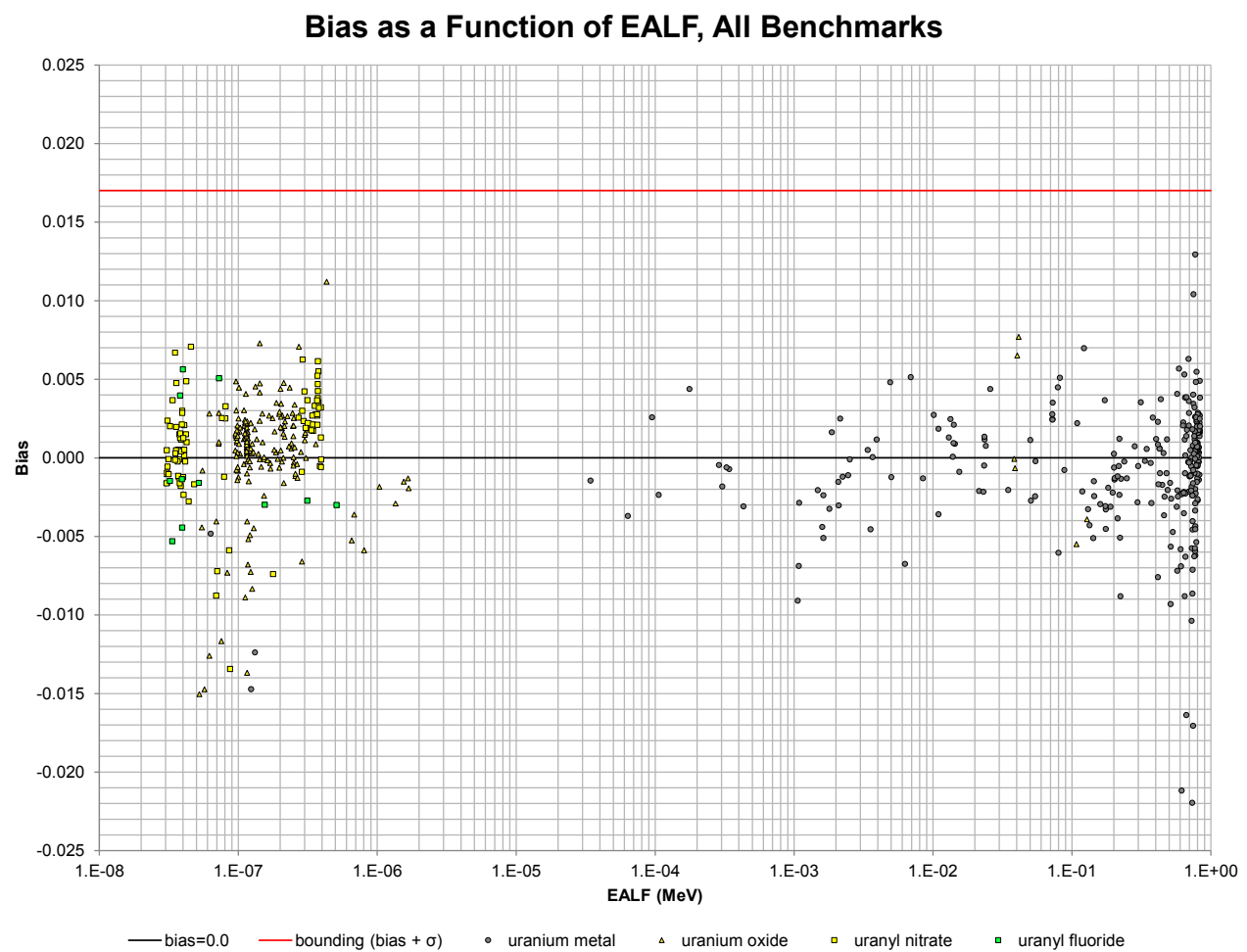


Figure A-16 – Bias as a Function of EALF, All Benchmarks

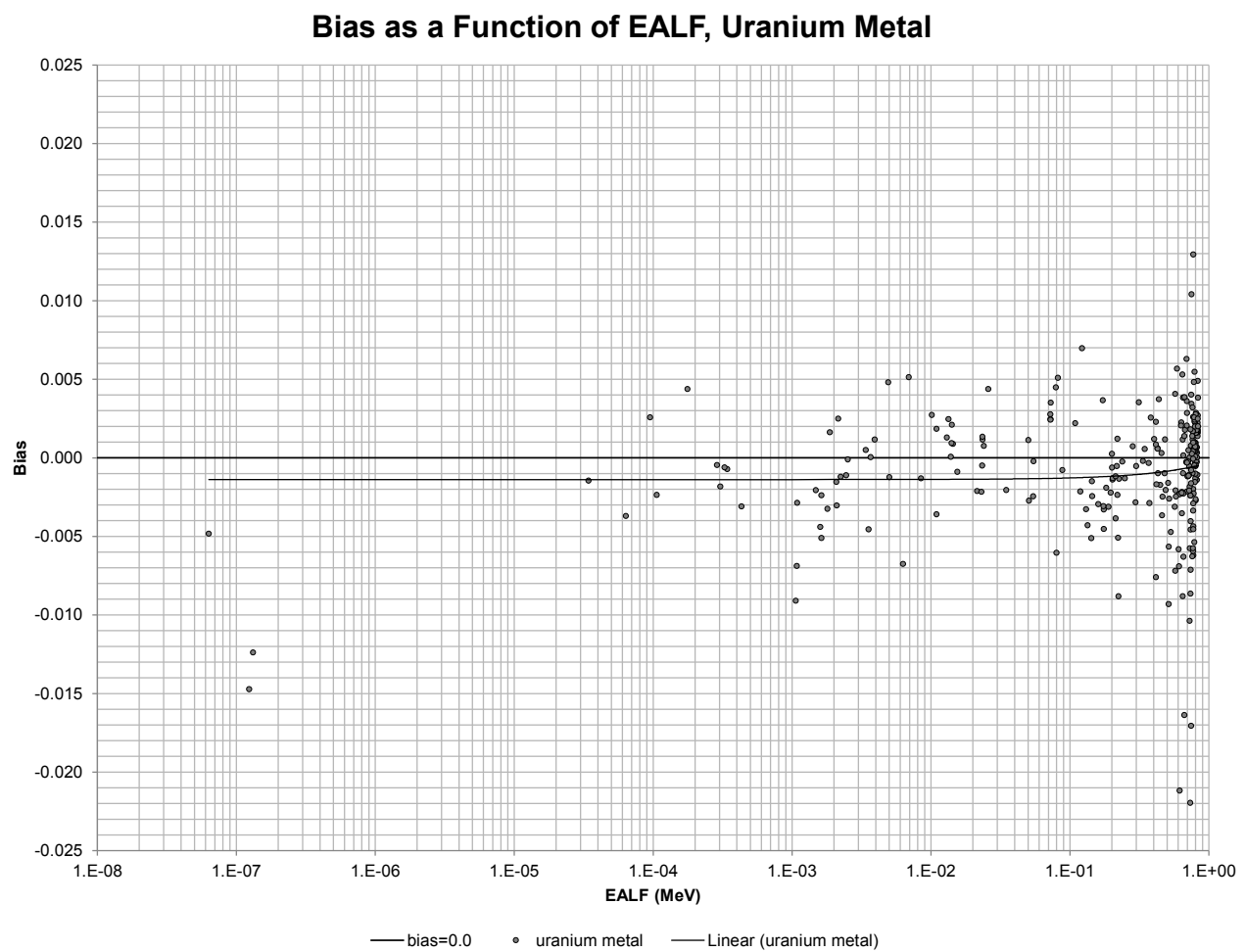


Figure A-17 – Bias as a Function of EALF, Metal Benchmarks

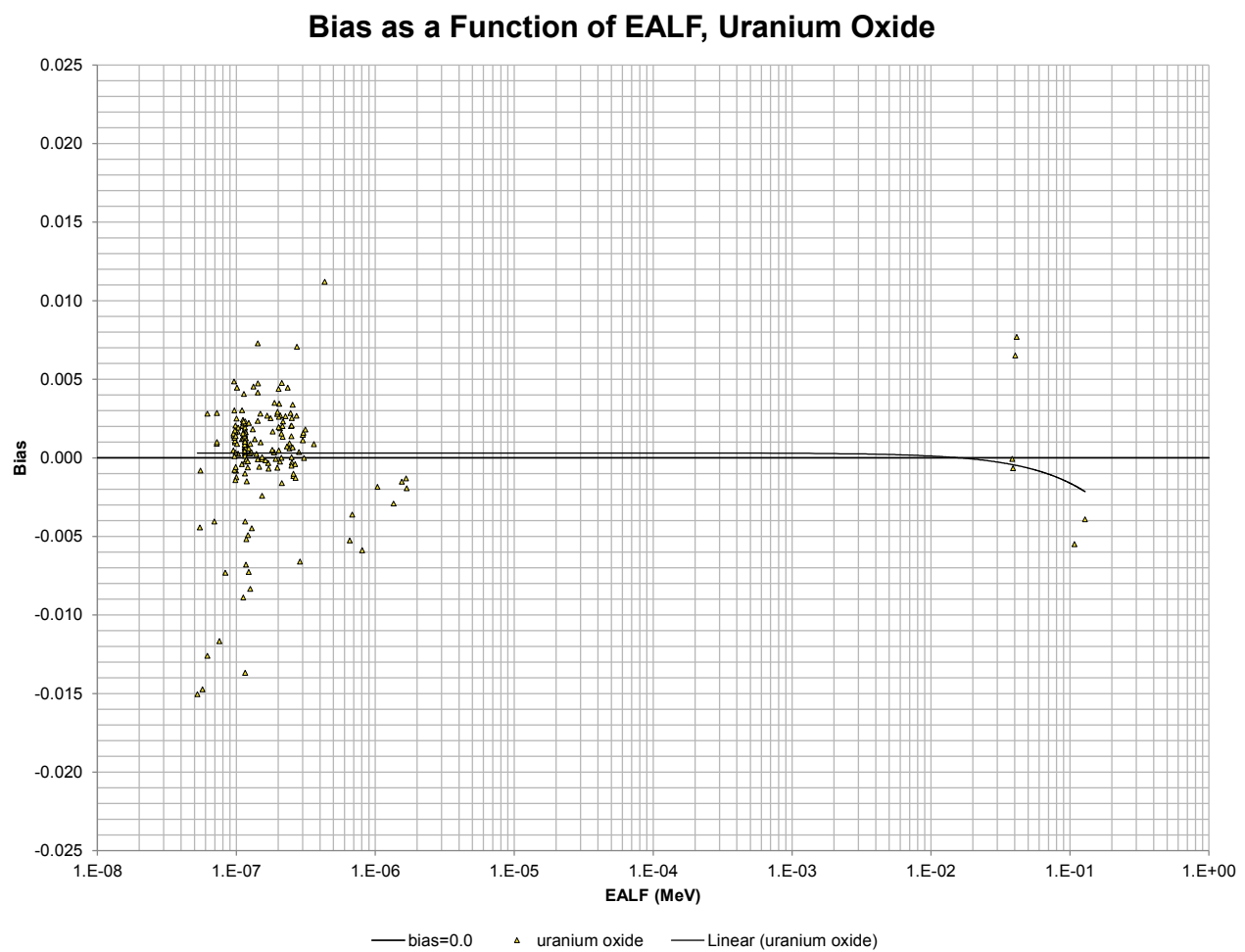


Figure A-18 – Bias as a Function of EALF, Oxide Benchmarks

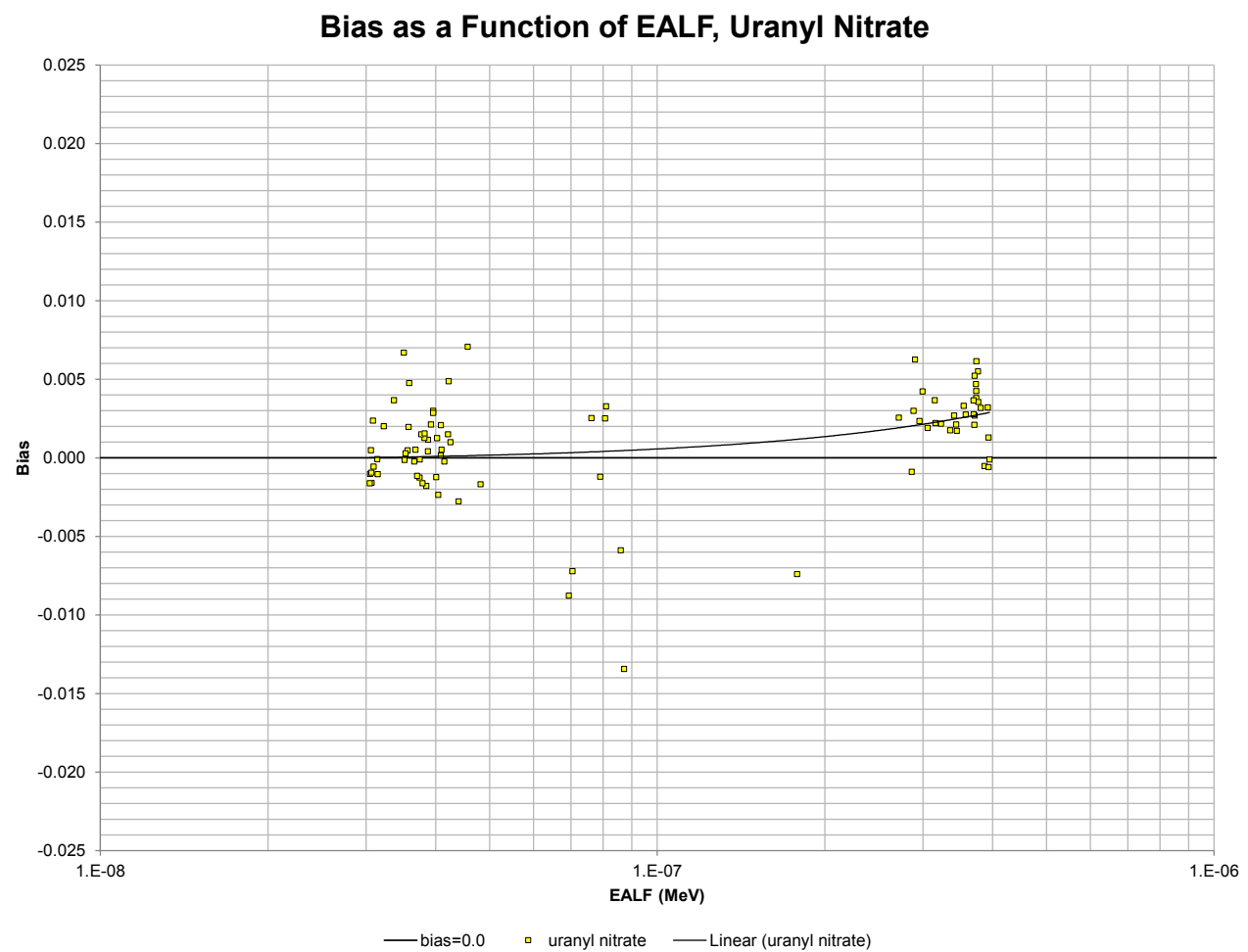


Figure A-19 – Bias as a Function of EALF, Nitrate Benchmarks

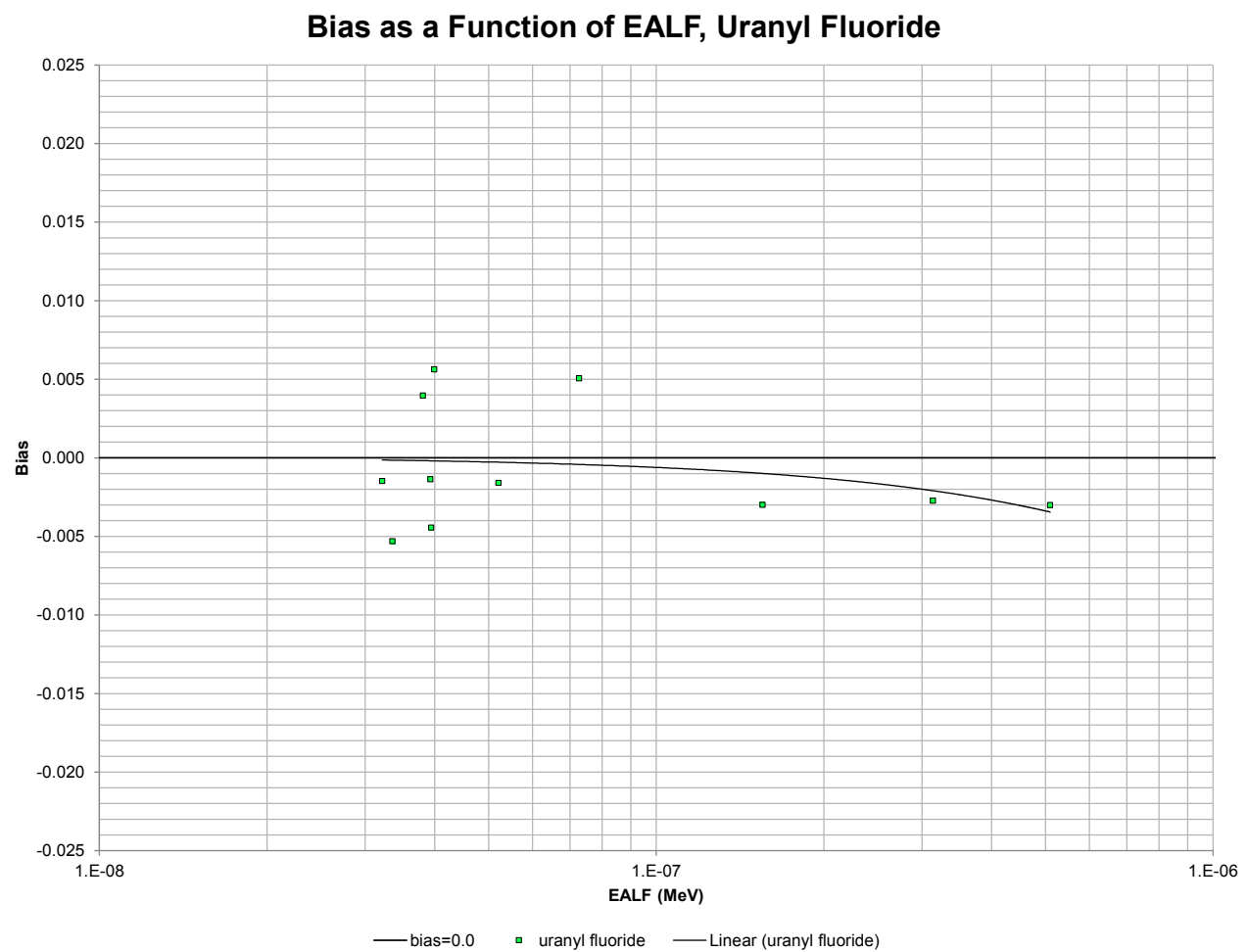


Figure A-20 – Bias as a Function of EALF, Fluoride Benchmarks

APPENDIX B – Chi-Squared Test Data

List of Tables

| | |
|--|----|
| Table B-1 – Chi-Squared Test for All Data | 38 |
| Table B-2 – Chi-Squared Test for Metal System Data | 38 |
| Table B-3 – Chi-Squared Test for Oxide System Data..... | 39 |
| Table B-4 – Chi-Squared Test for Nitrate System Data | 39 |
| Table B-5 – Chi-Squared Test for Fluoride System Data..... | 40 |

Table B-1 – Chi-Squared Test for All Data

| | | | | | | |
|-------------------|-----------|-----------|----------|----------|------------|-------------|
| mean | -0.000199 | | | | | |
| std dev | 0.003871 | | | | | |
| N | 556 | | | | | |
| p-value | 0.05 | | | | | |
| df | 9 | | | | | |
| P($Z \leq z_i$) | z(P) | x_lower | x_upper | observed | expected | $(O-E)^2/E$ |
| 0.1 | -1.282 | $-\infty$ | -0.0052 | 49 | 55.6 | 0.8 |
| 0.2 | -0.842 | -0.0052 | -0.0035 | 26 | 55.6 | 15.8 |
| 0.3 | -0.524 | -0.0035 | -0.0022 | 39 | 55.6 | 5.0 |
| 0.4 | -0.253 | -0.0022 | -0.0012 | 56 | 55.6 | 0.0 |
| 0.5 | 0.000 | -0.0012 | -0.0002 | 63 | 55.6 | 1.0 |
| 0.6 | 0.253 | -0.0002 | 0.0008 | 81 | 55.6 | 11.6 |
| 0.7 | 0.524 | 0.0008 | 0.0018 | 89 | 55.6 | 20.1 |
| 0.8 | 0.842 | 0.0018 | 0.0031 | 86 | 55.6 | 16.6 |
| 0.9 | 1.282 | 0.0031 | 0.0048 | 39 | 55.6 | 5.0 |
| 1.0 | | 0.0048 | ∞ | 28 | 55.6 | 13.7 |
| | | | | | $\chi^* =$ | 89.4 |
| | | | | | χ^2 | 16.9 |

Table B-2 – Chi-Squared Test for Metal System Data

| | | | | | | |
|-------------------|-----------|-----------|----------|----------|------------|-------------|
| mean | -0.000889 | | | | | |
| std dev | 0.004095 | | | | | |
| N | 272 | | | | | |
| p-value | 0.05 | | | | | |
| df | 9 | | | | | |
| P($Z \leq z_i$) | z(P) | x_lower | x_upper | observed | expected | $(O-E)^2/E$ |
| 0.1 | -1.282 | $-\infty$ | -0.0061 | 21 | 27.2 | 1.4 |
| 0.2 | -0.842 | -0.0061 | -0.0043 | 18 | 27.2 | 3.1 |
| 0.3 | -0.524 | -0.0043 | -0.0030 | 16 | 27.2 | 4.6 |
| 0.4 | -0.253 | -0.0030 | -0.0019 | 35 | 27.2 | 2.2 |
| 0.5 | 0.000 | -0.0019 | -0.0009 | 34 | 27.2 | 1.7 |
| 0.6 | 0.253 | -0.0009 | 0.0001 | 33 | 27.2 | 1.2 |
| 0.7 | 0.524 | 0.0001 | 0.0013 | 39 | 27.2 | 5.1 |
| 0.8 | 0.842 | 0.0013 | 0.0026 | 38 | 27.2 | 4.3 |
| 0.9 | 1.282 | 0.0026 | 0.0044 | 23 | 27.2 | 0.6 |
| 1.0 | | 0.0044 | ∞ | 15 | 27.2 | 5.5 |
| | | | | | $\chi^* =$ | 29.8 |
| | | | | | χ^2 | 16.9 |

Table B-3 – Chi-Squared Test for Oxide System Data

| | | | | | | |
|-------------------|----------|-----------|----------|----------|----------|-------------|
| mean | 0.000263 | | | | | |
| std dev | 0.003582 | | | | | |
| N | 186 | | | | | |
| p-value | 0.05 | | | | | |
| df | 9 | | | | | |
| P($Z \leq z_i$) | z(P) | x_lower | x_upper | observed | expected | $(O-E)^2/E$ |
| 0.1 | -1.282 | $-\infty$ | -0.0043 | 18 | 18.6 | 0.0 |
| 0.2 | -0.842 | -0.0043 | -0.0028 | 5 | 18.6 | 9.9 |
| 0.3 | -0.524 | -0.0028 | -0.0016 | 3 | 18.6 | 13.1 |
| 0.4 | -0.253 | -0.0016 | -0.0006 | 15 | 18.6 | 0.7 |
| 0.5 | 0.000 | -0.0006 | 0.0003 | 26 | 18.6 | 2.9 |
| 0.6 | 0.253 | 0.0003 | 0.0012 | 38 | 18.6 | 20.2 |
| 0.7 | 0.524 | 0.0012 | 0.0021 | 40 | 18.6 | 24.6 |
| 0.8 | 0.842 | 0.0021 | 0.0033 | 24 | 18.6 | 1.6 |
| 0.9 | 1.282 | 0.0033 | 0.0049 | 12 | 18.6 | 2.3 |
| 1.0 | 0.000 | 0.0049 | ∞ | 5 | 18.6 | 9.9 |
| | | | | | | $\chi^* =$ |
| | | | | | | 85.4 |
| | | | | | | χ^2 |
| | | | | | | 16.9 |

Table B-4 – Chi-Squared Test for Nitrate System Data

| | | | | | | |
|-------------------|----------|-----------|-----------|----------|----------|-------------|
| mean | 0.001041 | | | | | |
| std dev | 0.003271 | | | | | |
| N | 87 | | | | | |
| p-value | 0.05 | | | | | |
| df | 9 | | | | | |
| P($Z \leq z_i$) | z(P) | x_lower | x_upper | observed | expected | $(O-E)^2/E$ |
| 0.1 | -1.282 | $-\infty$ | -0.0032 | 5 | 8.7 | 1.6 |
| 0.2 | -0.842 | -0.0032 | -0.0017 | 3 | 8.7 | 3.7 |
| 0.3 | -0.524 | -0.0017 | -0.0007 | 12 | 8.7 | 1.3 |
| 0.4 | -0.253 | -0.0007 | 0.0002 | 10 | 8.7 | 0.2 |
| 0.5 | 0.000 | 0.0002 | 0.0010 | 7 | 8.7 | 0.3 |
| 0.6 | 0.253 | 0.0010 | 0.0019 | 9 | 8.7 | 0.0 |
| 0.7 | 0.524 | 0.0019 | 0.0028 | 17 | 8.7 | 7.9 |
| 0.8 | 0.842 | 0.0028 | 0.0038 | 12 | 8.7 | 1.3 |
| 0.9 | 1.282 | 0.0038 | 0.0052 | 7 | 8.7 | 0.3 |
| 1.0 | 0.000 | 0.0052 | $-\infty$ | 5 | 8.7 | 1.6 |
| | | | | | | $\chi^* =$ |
| | | | | | | 18.2 |
| | | | | | | χ^2 |
| | | | | | | 16.9 |

Table B-5 – Chi-Squared Test for Fluoride System Data

| | | | | | | |
|-------------------|-----------|-----------|----------|----------|----------|-------------|
| mean | -0.000756 | | | | | |
| std _dev | 0.003650 | | | | | |
| N | 11 | | | | | |
| p-value | 0.05 | | | | | |
| df | 9 | | | | | |
| P($Z \leq z_i$) | z(P) | x_lower | x_upper | observed | expected | $(O-E)^2/E$ |
| 0.1 | -1.282 | $-\infty$ | -0.0054 | 0 | 1.1 | 1.1 |
| 0.2 | -0.842 | -0.0054 | -0.0038 | 2 | 1.1 | 0.7 |
| 0.3 | -0.524 | -0.0038 | -0.0027 | 3 | 1.1 | 3.3 |
| 0.4 | -0.253 | -0.0027 | -0.0017 | 0 | 1.1 | 1.1 |
| 0.5 | 0.000 | -0.0017 | -0.0008 | 3 | 1.1 | 3.3 |
| 0.6 | 0.253 | -0.0008 | 0.0002 | 0 | 1.1 | 1.1 |
| 0.7 | 0.524 | 0.0002 | 0.0012 | 0 | 1.1 | 1.1 |
| 0.8 | 0.842 | 0.0012 | 0.0023 | 0 | 1.1 | 1.1 |
| 0.9 | 1.282 | 0.0023 | 0.0039 | 0 | 1.1 | 1.1 |
| 1.0 | 0.000 | 0.0039 | ∞ | 3 | 1.1 | 3.3 |
| $\chi^* =$ | | | | | | 17.2 |
| χ^2 | | | | | | 16.9 |

References

- 1 LA-UR-22934, 'Initial Release Overview – MCNP6 version 1.0', 04/24/2013 (Draft)
- 2 ANSI/ANS-8.1-2014, 'Nuclear Criticality Safety in Operations with Fissionable Materials Outside of Reactors'
- 3 ANSI/ANS-8.24-2007, 'Validation of Neutron Transport Methods for Nuclear Criticality Safety Calculations'
- 4 LA-UR-03-1987, 'MCNP – A General Monte Carlo N-Particle Transport Code, Version 5, Volume 1: Overview and Theory', 03/24/2003 (Revised 02/01/2008)
- 5 LA-UR-21878, 'Release of Continuous Representation for $S(\alpha,\beta)$ ACE Data', 03/20/2014
- 6 LA-UR-21822, 'Listing of Available ACE Data Tables', 2014-06-26 (rev.4)
- 7 LA-CP-13-00634, Rev.0, 'MCNP6 User's Manual', 05/2013
- 8 'md5sum.' Wikipedia: The Free Encyclopedia. Wikimedia Foundation, Inc. 22 July 2004. Web. 14 Dec. 2015. <<https://en.wikipedia.org/wiki/Md5sum>>
- 9 NCS-AP-0005, R1, 'NCS Software Quality Management', 08/19/2015
- 10 NEA/NSC/DOC(95)03, 'International Handbook of Criticality Safety Benchmark Experiments', September 2015
- 11 LA-UR-16-21302, 'MCNP Progress for NCSP', 2016-03-15
- 12 NUREG/CR-6698, 'Guide for Validation of Nuclear Criticality Safety Calculational Methodology'
- 13 'An Introduction to Error Analysis', Second Edition, John R. Taylor, ISBN 0-935702-75-X
- 14 NCS-GUIDE-01, R2, 'Criticality Safety Evaluations', 5/13/15